

Aus der
Klinik für Orthopädie und Unfallchirurgie
Klinik der Universität München
Direktoren: Prof. Dr. Wolfgang Böcker und Prof. Dr. Boris Holzapfel

**Influence of hypoxia and vascularization on the
osteogenic differentiation and mineralization capacity
of primary osteoporotic human mesenchymal stem cells**

Dissertation
zum Erwerb des Doktorgrades der Medizin
an der Medizinischen Fakultät
der Ludwig-Maximilians-Universität zu München

vorgelegt von
Céline Kohll

aus
Luxemburg

Jahr
2025

Mit Genehmigung der Medizinischen Fakultät
der Universität München

Berichterstatter: Prof. Dr. Wolfgang Böcker
Mitberichterstatter: PD Dr. Alexander C. Paulus
PD Dr. Volker Braunstein

Mitbetreuung durch die
promovierten Mitarbeiter: Dr. Maximilian Saller
Dr. Veronika Schönitzer
Dekan: Prof. Dr. med. Thomas Gudermann

Tag der mündlichen Prüfung: 08.05.2025

Abstract

The treatment of osteoporotic fractures that are associated with critical bone defects or non-unions is a significant clinical problem. To date, autografts have served as the gold standard for bone grafts. However, autografts have been associated with many risks. Bone tissue engineering (BTE) represents a potential alternative for the treatment of these complicated fractures. Although BTE research has largely improved, the translation into clinical applications has yet to be approved by regulatory agencies. As several companies have received approval for the use of intra-operation cell isolation systems, inadequate vascularization of scaffolds has been identified as a major problem. An additional concern is the reduced osteogenic differentiation potential of human mesenchymal stem cells (hMSCs) in elderly patients. Therefore, many research groups have examined how to improve vascularization and osteogenic differentiation potential. One widespread approach for manufacturing prevascularized scaffolds has been a co-culture of scaffolds with hMSCs and human umbilical vein endothelial cells (hUVECs) combined with the testing of different oxygen levels in cell culture. The aim of the present study was therefore to gain knowledge about the influence of oxygen on the proliferation, growth characteristics, and osteogenic differentiation of hMSCs from different donors, specifically patients with high-energy fracture trauma (HET) and osteoporotic fracture trauma (OFT). Furthermore, co-cultures from donors of the HET group and OFT group with hUVECs, undergoing osteogenic differentiation were analyzed. For this study, hMSCs were isolated from different donor sites and randomized into the two donor groups HET or OFT. Initially, the morphology, growth characteristics, proliferation (Cumulative Population Doubling and colony forming units (CFU)) and osteogenic differentiation potential of hMSCs in normoxia and hypoxia were analyzed. Further, the osteogenic differentiation potential of co-cultures (hMSCs:hUVECs) in different ratios was tested in 2D and 3D.

Analysis of the morphology aspect in hypoxia and normoxia showed a tendency towards flattening of the cells for both groups (HET and OFT) in normoxia. Following cumulative population doubling in normoxia versus hypoxia, both groups showed a non-significant tendency toward improved proliferation in hypoxia. Further osteogenic differentiation was examined, showing that osteogenic differentiation in hypoxia was non-significantly reduced for both groups (HET and OFT). Comparison of the two groups, HET and OFT, found that the proliferation capacity, CFU capacity, and osteogenic differentiation potential of the HET group had a tendency towards better performance, although that difference was not always significant. Further co-cultures (hMSCs:hUVECs) of different ratios (1:0, 1:2, 1:3) were analyzed to gain a better understanding of the interaction between the cell types and the osteogenic differentiation potential in co-cultures. Most donor samples showed a tendency towards a higher osteogenic differentiation capacity in co-cultures than in hMSCs monocultures. The influence of the co-culture was more pronounced for OFT hMSCs than for the HET hMSCs.

Although many results were non-significant, a tendency towards improved proliferation and later senescence in hypoxia, stronger osteogenic differentiation capacity in normoxia and a better osteogenic differentiation capacity in co-cultures demonstrates that hMSCs are very sensitive to oxygen levels and their behavior is influenced by co-cultures. The knowledge of the specified pathways behind these interactions and the best conditions for hMSCs and hUVECs still have to be investigated. All these findings will help identify a better solution for non-union fractures and improve BTE.

Abstract

Die Behandlung von osteoporotischen Frakturen, die mit kritischen Knochendefekten einhergehen, stellt ein erhebliches klinisches Problem dar. Bislang gelten Autotransplantate als Goldstandard für Knochentransplantate, diese sind jedoch mit vielen Risiken behaftet. Bone Tissue Engineering (BTE) stellt eine mögliche Alternative für die Behandlung dieser komplizierten Frakturen dar. Die BTE-Forschung hat sich bereits extrem weiterentwickelt, jedoch fehlt für die Umsetzung in die klinische Anwendung noch oft die Zulassung durch die Aufsichtsbehörden. Einige Unternehmen haben die Zulassung für intraoperative Zellisolationssysteme erhalten und die unzureichende Vaskularisierung sowie reduzierte osteogene Differenzierungskapazität von humanen mesenchymalen Stammzellen aus älteren Spendern als ein großes Problem identifiziert. Ein weit verbreiteter Ansatz zur Herstellung solcher Systeme ist die Ko-Kultur von mit humanen mesenchymalen Stammzellen (hMSCs) und humanen Nabelvenenendothelzellen (hUVECs). Allerdings stellt die Bildung funktioneller Gefäße und eine ausreichende osteogene Differenzierung eine Herausforderung dar. Ziel der vorliegenden Studie war es daher, Erkenntnisse über den Einfluss von Sauerstoff auf die Proliferation, die Wachstumseigenschaften und die osteogene Differenzierung humaner mesenchymaler Stammzellen (hMSCs) von verschiedenen Spendern zu gewinnen. Darüber hinaus wurden Ko-Kulturen mit hMSCs und hUVECs aus beiden Gruppen (HET und OFT) und deren osteogene Differenzierung und Zellveränderung analysiert.

hMSCs wurden aus verschiedenen Spenderstellen isoliert und randomisiert in zwei Spendergruppen eingeteilt, die entweder ein hochenergetisches Frakturtrauma (HET) oder ein osteoporotisches Frakturtrauma (OFT) erlitten hatten. Zunächst wurden Morphologie, Proliferation, Wachstumseigenschaften von hMSCs unter Normoxie und Hypoxie analysiert. Beide Gruppen zeigten eine nicht signifikante, jedoch tendenziell bessere Proliferation unter Hypoxie. Bei näherer Betrachtung der morphologischen Veränderungen unter Hypoxie und Normoxie zeigte sich, dass die Zellen unter Hypoxie weniger angeflacht erschienen. Das osteogene Differenzierungspotential zeigte sich in der Hypoxie reduziert im Vergleich zur Normoxie. Vergleicht man das Differenzierungspotenzial der HET-Gruppe mit dem der OFT-Gruppe, so zeigten die meisten Spender der HET-Gruppe ein höheres Proliferationspotenzial und Differenzierungspotenzial als die OFT Spender. Des weiteren wurden Ko-Kulturen von hMSCs und hUVECs in verschiedenen Verhältnissen (1:0, 1:2, 1:3) angesetzt und das osteogene Differenzierungspotenzial analysiert. Die meisten Spender zeigten eine höhere osteogene Differenzierungskapazität unter der Ko-Kultur als in der Monokultur. Bei der Analyse der verschiedenen Spender zeigte sich, dass der Einfluss der Ko-Kultur bei den OFT hMSCs stärker ausgeprägt war als bei den HET hMSCs.

Auch wenn viele Ergebnisse nicht signifikant waren, zeigte sich eine Tendenz zu einer besseren Proliferation und späteren Seneszenz unter Hypoxie. Einer höheren osteogenen Differenzierungskapazität unter Normoxie und einer besseren osteogenen Differenzierungskapazität in Ko-Kulturen. Die Tatsache, dass hMSCs aus der OFT-Gruppe stärker von Ko-Kulturen beeinflusst wurden als hMSCs aus der HET-Gruppe, zeigt, dass es noch einige Signalwege oder wichtige Gene zu entdecken gibt. Das Wissen über die spezifischen Wege hinter diesen Interaktionen und die besten Bedingungen für hMSCs und hUVECs sollten noch weiter erforscht werden um BTE zu verbessern.

Contents

1	Introduction	1
1.1	Osteoporosis	1
1.2	Bone tissue	2
1.2.1	Bone development	2
1.2.2	Vascular system and oxygenation in the bone	3
1.2.3	Bone matrix	5
1.3	Bone fracture healing	6
1.3.1	Bone regeneration	6
1.3.2	Treatment of non-union bone defects	6
1.4	Regenerative medicine	7
1.4.1	Development and possibilities of bone tissue engineering	7
1.4.2	The role of vascular development and oxygen supply for tissue engineering	7
1.5	Cell lines used in regenerative medicine	8
1.5.1	Mesenchymal stem cells	8
1.5.2	Umbilical vein endothelial cells	8
1.6	Aim of the study	9
2	Materials and Methods	10
2.1	Cell material	10
2.2	Isolation and expansion of donor cells	10
2.3	Cell counting.....	10
2.4	Thawing and cultivation of cells.....	11
2.5	Trypsinization and cryopreservation	11
2.6	Cumulative population doubling and population doubling time	12
2.7	Morphological changes.....	12
2.8	Colony forming units and alkaline phosphatase activity	12
2.9	Osteogenic differentiation.....	13
2.10	Alizarin Red staining and quantification	14
2.11	3D seeding of a collagen scaffold with monocultures of hMSCs and co-cultures of hMSCs/hUVECs	14
2.12	Determination of cell survival using life-death-assay	15
2.13	Statistical analysis	15
3	Results	17
3.1	Hypoxia maintains cell morphology and proliferation over time	17
3.1.1	Cell morphology	17
3.1.2	Cumulative population doubling	19
3.1.3	Colony forming units.....	23
3.2	Osteogenic differentiation potential of the HET group and OFT group in normoxia and hypoxia	24
3.3	Co-culture of hMSCs and hUVECs enhance osteogenic differentiation capacity	27
3.4	hUVEC survival and morphology changes under co-cultures .	32
4	Discussion	33
4.1	Biological cell characteristics	33
4.1.1	Cell morphology	33
4.1.2	Proliferation of hMSCs in different oxygen levels	34
4.2	Osteogenic differentiation potential in different oxygen concentrations	35

4.3	Osteogenic differentiation potential in co-culture	36
4.4	Morphological changes of hUVECs and their role in bone tissue engineering	37
4.5	Critical discussion of the experimental setup	38
5	Conclusion and Outlook	38
6	References	40
7	Supplementary data	52
7.1	A. Influence of the donor age on proliferation, colony forming unit capacity and osteogenic differentiation capacity	52
8	Appendix	54
8.1	List of materials and chemicals	55
9	Acknowledgments	64
10	Eidesstattliche Versicherung	65
11	Erklärung zur Übereinstimmung der gebundenen Ausgabe der Dissertation mit der elektronischen Fassung	66

1 Introduction

1.1 Osteoporosis

Osteoporosis is a common disease of the skeleton that becomes more prevalent with advancing age. Osteoporosis has been defined as “*a systemic skeletal disease characterized by low bone mass and micro-architectural deterioration of bone tissue with a consequent increase in bone fragility and susceptibility to fracture*” [1]. The treatment of osteoporosis has become even more important with the current demographic changes. Osteoporotic fractures have a high morbidity and mortality, for women the risk of dying from a hip fracture is almost equivalent to the risk of dying from breast cancer [2]. This health risk highlights the growing importance of this subject. Given its rising prevalence, osteoporosis has become a major public health issue, resulting in a greater need for medical care and an augmentation of the associated costs [3–5].

There are two common primary causes of osteoporosis: postmenopausal osteoporosis and age-related osteoporosis. Secondary causes can be due to immobilization, alcohol abuse, hyperparathyroidism, hypercortisolism or any disease that interacts with the bone physiology [6].

Various diagnostic methods and treatment options have evolved over the years. The most common method for diagnosing osteoporosis has been the measurement of bone mineral density (BMD), which also reflects an assessment of the outcome of treatment modalities [7]. One of the main pillars in the assessment of osteoporosis is bone densitometry, which can be measured by dual x-ray absorptiometry (DXA); quantitative ultrasound (QUS) and quantitative computed tomography (qCT) have been used less frequently [8–10]. DXA has become the most common technique used to determine BMD. Based on the obtained BMD values, T- or Z-scores are calculated, both of which are entities of standard deviation (SD). The T-score is defined as “*the number of SDs by which the BMD in an individual differs from the mean value expected in young healthy individuals*” [7]. A T-score of SD „, -2.5 to the female adult mean has been defined as osteoporosis. Severe osteoporosis would mean that one or more fragility fractures are present [11].

The clinical importance of osteoporosis is due to the accompanying fractures and their influence on morbidity and mortality. As fracture risk has been related to skeletal and non-skeletal (e.g. liability to fall) components, it is imperative to adopt a broad approach in the assessment of fracture risk, thus accounting for all components. Different aspects, such as the DXA, the biochemical assessment and the clinical risk factors, must be considered. DXA measurement can be used to differentiate between a normal and an osteoporotic BMD. A normal BMD does not guarantee a total absence of fracture risk, although the risk is minimized in this case. Conversely, osteoporosis does not mean that a fracture will certainly occur [11]. In the biochemical assessment of fracture risk, different markers for formation (e.g. total alkaline phosphatase and osteocalcin) and resorption (e.g. hydroxyproline) are examined. Correlations between osteoporotic fractures and levels of bone turnover markers have been established in different studies [2, 12]. Therefore, a combination of BMD and bone markers might improve fracture prediction risk [11]. The clinical risk factors must be acknowledged as well. Diseases such as hypogonadism and hyperprolactinemia, chronic illness, alcohol and cigarette abuse and premature menopause, among many other factors, have been associated with a higher risk of osteoporosis [13, 14].

Based on the many factors influencing a fracture prediction, a computer-based algorithm, named fracture risk assessment tool, which calculates an estimation of a 10-year probability for a major fracture. Different inputs, such as age, body mass index, alcohol consumption and long term oral glucocorticoid treatment are used to calculate this fracture risk. The results are categorized as low, high, or very high risk, and treatment can be adapted accordingly [15].

Along with the diagnosis comes the treatment and the prevention of osteoporosis. Osteoporotic individuals undergo either pharmacological or non-pharmacological treatment. Additionally, lifestyle changes should be considered for any osteoporotic patient. A healthy diet with a regulated calcium, vitamin D and protein (1g/kg/day) intake [16], as well as regular muscle-strengthening exercises, alcohol and tobacco abstinence and fall prevention should be implemented. For patients with a high fracture risk, pharmacological treatment is essential [7]. The most essential drugs can be divided into two major groups: anti-resorptive drugs (bisphosphonates, selective estrogen-receptor modulator (SERM) and antibody therapy with Denosumab) and anabolic agents (teriparatide and romosozumab) [16–21].

On a cellular level, osteoporosis is marked by an imbalance of activity between osteoblasts and osteoclasts, which is dominated by osteoclasts. This results in a higher resorption and removal of bone than bone formation [21]. Unfortunately, the exact mechanism has yet to be fully elucidated. There have been many studies analyzing osteoporotic bone structures. Studies in humans and mice have suggested that a malfunction of osteoclasts might be one of the reasons for osteoporosis [22]. Another hypothesis is the replacement of bone marrow by adipocytes due to the impaired differentiation potential of mesenchymal stem cells at the expense of osteogenesis [23–26]. Moreover, the decreased bone mass in older patients related to a minimized vascularization and blood flow, might be due to changes in the composition and number of H- and L-vessels as well as a reduction of the total number of arteries [27, 28]. Such changes in bone biology inhibit bone healing and can cause critical-size bone defects which are inherently difficult to repair. Therefore, different treatments have been and are in the process of being tested, with bone tissue engineering (BTE) at the forefront. To completely understand the fundamentals of bone tissue engineering (BTE), it is important to understand bone tissue.

1.2 Bone tissue

1.2.1 Bone development

Bone tissue has different structural and mechanical properties acquired due to its micro- and macro structural architecture. There are different types of bone, woven and lamellar bone on a microscopic level and trabecular and cortical bone one a macroscopic level [29].

The process of bone formation, so-called ossification, has been divided into two different types: intramembranous and endochondral ossification. [30] Proliferation, development and mineralization are the pivotal stages of ossification, in which a complex balance between vascularization, oxygenation, apoptosis and signaling pathways is obligatory for active bone formation. Prior to ossification, mesenchymal cells that are derived from embryonic lineages migrate and build cell depositions, thereby predetermining the future bone structure [31]. From this structure, both ossification types can

develop, depending on whether cells transform into osteoblasts or chondrocytes [32].

Intramembranous ossification is a direct process without interim cartilage formation. Mesenchymal stem cells differentiate into osteoblasts and osteogenic cells to form primary ossification centers (POC). Mature lamellar bone is formed through maturing and mineralizing of the bone matrix. The formation of the maxilla and skull base is mainly a result of intramembranous ossification. [33, 34].

Endochondral ossification, which is responsible for the majority of the human skeleton (e.g. tibia, femur and humerus), is a more complex process. After progenitor cells differentiate into chondrocytes, they build a cartilage architecture with the shape of the future bone. [35] Hypertrophic changes in chondrocytes followed by the invasion of osteogenic progenitor cells, connective tissue and blood vessels support bone development and primary ossification centers are developed [36]. The supply of nutrients and oxygen through capillaries is important for the stimulation of the osteoprogenitor cells. Starting with the resorption of the hypertrophic cartilage and the formation of bone marrow through the interaction of different cell types (osteoblast progenitors, endothelial and hematopoietic cells), primary ossification centers are formed [37]. Due to growth, secondary ossification centers (SOC) occur and the processes of mineralization, apoptosis of chondrocytes, invasion of capillaries and proliferation of osteogenic cells transforming into osteoblasts repeat themselves. Over time, epiphyseal growth plates will develop and contribute to the longitudinal growth of the bone [32, 38]. Growth plates are comprised of different zones (proliferative, prehypertrophic and hypertrophic apoptotic) where cartilage is transformed into bone matrix [39]. Over a lifetime, bone modeling (formation of new bone) and remodeling (replacement of old bone) occur repeatedly, with influence from mechanical, physiological and hormonal factors [40].

1.2.2 Vascular system and oxygenation in the bone

The vascular system and oxygenation are indispensable for bone development and remodeling. Vasculature is the primary source of oxygen, growth factors and hormones and is essential for bone formation. Several animal studies have suggested that approximately 10-15% of the total cardiac output is used by the skeletal system [41]. No exact data on oxygen concentrations in human bone has been found. Nonetheless, studies have suggested oxygen concentrations of 1-6 % in the bone marrow tissue [42] and 5-12.5% in the bone tissue [43, 44]. An unbalanced or undeveloped vascular system can result in severe skeletal diseases, such as craniofacial dysmorphology or idiopathic osteonecrosis [45, 46].

Vasculogenesis and angiogenesis are two different types of blood vessel formation. Vasculogenesis refers to the development of a blood vessel from mesenchymal stem cells, hemangioblasts, or angioblasts [47], whereas angiogenesis describes the development of a new blood vessel from a pre-existing vessel [48].

Vasculogenesis and angiogenesis already occur in the early stages of embryonic development. The production of vascular endothelial growth factor (VEGF) is pivotal in both types of ossification. Transcription factors, such as runt-related transcription factor 2 (RUNX2) and osterix, which are

produced by progenitor cells or hypertrophic chondrocytes, induce the expression of VEGF. VEGF stimulates the Notch pathway through increased expression of the Notch ligand Delta-4, causing guided sprouting of angiogenesis [27]. VEGF couples osteogenesis and angiogenesis, by stimulating endothelial cells and consequently inducing angiogenesis (Figure 1). This, causes an increased supply of nutrients, oxygen and infiltration of progenitor cells, which are essential for bone formation. Moreover, angiogenesis causes increased levels of endothelium-derived osteogenic growth factors, such as bone morphogenetic protein 4 (BMP4) and bone morphogenetic protein 2 (BMP2), thereby influencing the function of osteoblasts and osteoclasts [49, 50].

In the center of the epiphyseal growth plate, a lack of oxygen, nutrition and growth factors (insulin-like-growth-factor 1 (IGF-1)), activates the hypoxia-inducible factor (HIF) pathway. HIF is an $\alpha\beta$ transcription factor that plays an important role in the adaptation of cells to oxygen changes. HIF consists of different alpha subunits (HIF-1 α , HIF-2 α and HIF-3 α). In hypoxic conditions, the HIF-1 α subunit gathers in the cell and is transported to the nucleus, where it heterodimerizes with the HIF-1 β subunit. The dimer subsequently influences hypoxia responsive genes through the binding of different elements [51]. The HIF pathway is activated in the hypoxic environment of the growth plate causing an increased formation of angiogenic factors (e.g. VEGF, angiopoietin-1, angiopoietin-2) by chondrocytes [52]. Additionally, HIF-1 α is important for the survival of chondrocytes and induces the expression of membrane type-1 matrixmetalloproteinase. This causes cartilage degradation and thus facilitates the ingrowth of vessels [27, 39, 53].

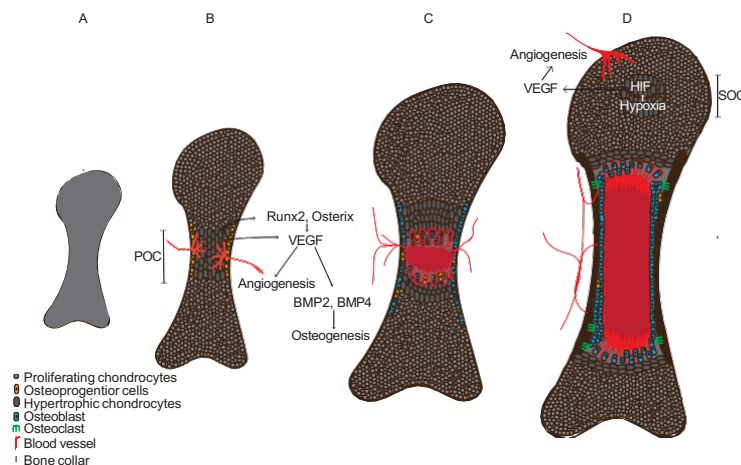


Figure 1: Schematic overview of the development of the bone and vascular system. A. Progenitor cells differentiate into chondrocytes and form a cartilage model with the shape of the future bone. B. Chondrocytes in the center become hypertrophic and mesenchymal stem cells in the perichondrium differentiate into osteoprogenitor cells, forming the primary ossification center (POC). Osteoprogenitor cells and chondrocytes increase VEGF expression through transcription factors (Runx2 and Osterix). VEGF stimulates the neovascularization of the cartilage model. The invasion of new blood vessels increases the supply of oxygen, nutrients and growth factor, thereby promoting mineralization. C. With the invasion of the blood vessels, osteoprogenitors move along to the changing site. Cartilage is resorbed by osteoclasts and new bone is formed by osteoblasts. With the ongoing process, a bone marrow cavity is produced. Concurrently, the epiphyseal growth plates, which are responsible for longitudinal growth, are formed. Perichondrium is transformed into periosteum. D. Due to the longitudinal growth and the avascularity of the growth plate, cells encounter a hypoxic state. The latter causes the stabilization of HIF and increases the expression of VEGF by chondrocytes. The invasion of vessels, which contribute to the formation of a secondary ossification center (SOC), is facilitated.

Macroscopically, three major parts of the vascular system have been identified: the central nutrient artery, the metaphyseal and epiphyseal arteries and the periosteal artery [45]. Microscopically, the Haversian and Volkmann's canals contain the vessels, which are built by different types of cells, mostly endothelial cells. Vessels are presented by two different types, H and L, which differ concerning HIF1-a. Type-H cells, which are mostly located in the metaphysis and near the endosteum, express higher levels of HIF1-a and CD31/endomucin compared to type-L cells, which are located in the sinusoids [22, 27, 54, 55].

To understand age-related bone pathologies such as osteoporosis, it is important to assess vascular changes in the bone. Age has been shown to cause a malfunctioning of the remodeling processes of vascularization in multiple ways, leading to insufficient tissue perfusion and thus organ function. Alterations in the circulation of pro- and anti-angiogenic factors, nitric oxide (NO) availability and bioenergetic pathways (e.g. NAD+ pathway) are at the root of microvascular rarefaction [56]. It has been shown that there is a correlation between decreased bone mass and decreased skeletal blood flow [57]. Recent studies have suggested that decreasing blood flow, followed by decreasing bone mass, can be explained by changes in the function and phenotype of endothelial cells in bone vessels. Experiments in aged mice (70 weeks old) have shown that the number of arterioles, especially type-H vessels, dramatically decreases with age. Furthermore, a downregulation in Notch signaling causes a reduced blood flow [28].

1.2.3 Bone matrix

Bones have a pivotal role in protecting organs, providing support, stability and participating in the mineral homeostasis. They are represented mostly by two types: trabecular (cancellous) and cortical (compact) bone, differing in structure and porosity [29]. The interaction between osteoclasts, osteoblasts, osteocytes, osteogenic cells and bone lining cells causes constant remodeling of the skeleton. Each of these cells has special functions in regarding bone turnover and is responsible for building and removing bone matrix [58].

Bone matrix is built of three different types of materials: 60% inorganic material, 30% organic material and 10% water. The organic component, also called osteoid, is composed mostly of collagen type I (more than 90 %) as well as over 30 other non-collagenous proteins (e.g growth factors, cytokines) and 2% bone-resident cells [59]. The roles of the non-collagenous proteins have not been clearly identified, but they are believed, to be essential for the interaction between osteoblasts and osteoclasts. Collagen type I has a triple-helical shape, formed by three polypeptide chains, two alpha-1 and one alpha-2 chain. These chains are cross-linked and form a linear molecule (300nm length), which bundles into collagen fibrils. The latter then groups to form a collagen fiber, building a framework for the mineralization process [60]. Osteoid is synthesized and secreted via osteoblasts, which also cause phosphate to deposited into the collagen framework. Within the collagen framework phosphate binds with calcium from the extracellular fluid and is hardened by bicarbonate and hydroxide ions, forming hydroxyapatite crystals $[Ca_3(PO_4)_2]_3Ca(OH)_2$. Several factors, such as hormones, bone morphogenetic proteins and wingless signaling pathways, dictate the function and differentiation of osteoblasts. [58, 61, 62]

A balance between organic and inorganic components is very important to sustain flexibility and stability in the bone. Osteoclasts are another

important cell type to ensure this balance. Deriving from the monocyte macrophage lineage, osteoclasts have the capacity to resorb bone [63]. Cytokines, such as receptor activator of NF- κ B ligand (RANKL) and colony-stimulating factor 1 are important for the stimulation and differentiation of pre-osteoclasts and are secreted by osteoblasts, osteocytes and immune cells [64]. Osteocytes descend from osteoblasts and are surrounded by osteoid. Osteocytes comprise 95% of all bone cells and are located in lacunae. Long dendritic processes enable communication with other osteocytes and osteoblasts to regulate the remodeling process [40, 65]. The fourth cell type is bone lining cells, which cover bone surfaces. To date, the role of lining cells remains unclear, although several studies have demonstrated their influence on osteoclast differentiation and the capacity to produce RANKL and osteoprotegerin (OPG), causing a decrease in bone remodeling [66,67].

1.3 Bone fracture healing

1.3.1 Bone regeneration

After a fracture or injury in mature bones, it takes three to six months to fully regain the previous bone structure and strength [68]. The healing process occurs in three consecutive steps: inflammation, repair and remodeling of the bone [69].

The inflammatory response is defined by the formation of a hematoma accompanied by inflammatory-associated cells (neutrophils and macrophages). These cells release cytokines (e.g. interleukin-1 (IL-1), interleukin-6 (IL-6)), tumor necrosis factor-alpha (TNF- α) and growth factors, after which nearby mesenchymal stem cells migrate and differentiated into angioblasts, chondroblasts, fibroblasts, and osteoblasts. Fibroblasts and osteoblasts produce granulation tissue in order to fill the gap [70].

The repair stage starts with the resorption of necrotic bone fragments by osteoclasts. Osteoclasts influence angiogenesis by producing heparinase, an enzyme responsible for the release of VEGF from heparin [39]. The new osteoid, also called callus, is formed by osteoblasts. Chondrocytes, located in the hypoxic areas of the fracture, produce cartilage, which in turn is replaced by endochondral bone ossification. As the vascular system around the fracture site is compromised and metabolic demand is elevated, oxygen concentrations can decrease to 1% O₂ [43]. The hypoxic environment activates the HIF- α pathway and induces angiogenesis [27, 41]. The final stage is marked by remodeling and reshaping of collagen fibers and dispersing crystals into woven bone, which is the predecessor of lamellar cortical bone. The interaction between osteoclasts resorbing woven bone, and osteoblasts forming lamellar bone is responsible for the restoration of bone shape, structure and mechanical strength [71–73].

1.3.2 Treatment of non-union bone defects

A bone fracture is defined as a continuity loss of bone structure and can be divided into different categories of severity. A fracture with a healing process exceeding six months is referred to as non-union fracture [68]. In the case of a bone defect larger than 6 mm (critical-size bone defect), the body cannot repair the damage on its own [74, 75]. Bone fractures can be caused by degenerative diseases or accidents and are followed by healing and remodeling processes. The remodeling process depends on different cell types,

vascularization, oxygen, cytokines and other mediators. Defect size or insufficiency of the remodeling system can inhibit full re-establishment of bone integrity. In this case, up-to-date bone grafts are the gold standard. Two different types, autografting or allografting, are possible, whereby the former is more common. In autografting, bone tissue is extracted from the patient's own body and implanted at the affected site. This guarantees low rejection rates and good biocompatibility. The downsides of autografting are donor site morbidity and size limitation, resulting in only small size defect treatment. Allografts are extracted from a donor body, delivering potentially more tissue, and thus the possibility of treating larger defects. Unfortunately, the procedure has been restricted due to donor availability, risk of disease transmission and a higher rate of immunogenic reactions [76–78].

1.4 Regenerative medicine

1.4.1 Development and possibilities of bone tissue engineering

Given the limitations of autogenic and allogenic bone grafts, many research teams have been developing new methods to treat non-union fractures, with BTE comprising the majority of the research. BTE covers a vast field of methods and materials used to replace or repair bone tissue by implementing a scaffold as a supportive environment.

To promote regeneration, the composition and proprieties of the scaffold are of importance. Roughness, porosity, chemical composition, biocompatibility and internal architecture, all define the effectiveness of a scaffold. Widely used materials include collagen, fibrin, gelatine, silk sericin and several polysaccharides such as hyaluronic acid [79]. Scaffolds should have the ability to induce osteoinduction, osteogenesis and osteointegration [77]. Different processes, such as gas foaming (GF), cryotropic gelation, additive manufacturing (binder jetting and powder bed fusion), vat photopolymerization, electrospinning and bioprinting have been researched [74]. Bioprinting offers the possibility to print temporary extracellular matrixes with directly embedded regenerative cells. The shape design of printed temporary extracellular matrixes is very flexible and therefore easily customized [79]. For a successful implantation of a scaffold, the interaction with MSCs, which need to adhere to and proliferate within the scaffold, is essential. An improved environment for bone cells and angiogenesis is provided by inducing a mineralization process with a gradient from the outside to the inside of the scaffold [77,80,81]. Few scaffolds have been tested clinically, examples include one 3D printed by Saijo et al. [82] for the purpose of maxillofacial plasty in 20 patients and a biphasic calcium-phosphate scaffold for the treatment of partial and total edentulism by Luongo et al. [83] Both studies treated only small defects.

1.4.2 The role of vascular development and oxygen supply for tissue engineering

One of the biggest problems yet to be solved in BTE, is the vascularization of the scaffolds. For large bone defects in particular, scaffolds need to be of a certain size, making vascularization complicated and thus causing a hypoxic environment in the center of the scaffold. It has been shown that oxygen is only diffused from a blood vessel for 150-200 μ m, disabling MSCs to adapt their glucose metabolism and resulting in MSCs dying within three days [84, 85]. Therefore, angiogenesis and vasculogenesis must evolve quickly to ensure the supply of oxygen and nutrients, desperately needed

for cell survival and metabolism. Different approaches developing scaffolds with functional vascular networks have already been tested. The ingrowth of a vascular network of the host into the scaffold, faces the problem that neo-angiogenesis takes $\sim 5\mu\text{m}/\text{h}$, conducting to a hypoxic environment inside the scaffold for a prolonged time. Building a vascular scaffold within the pre-seeded scaffold that will connect with the host vascular system once implanted has also been tested. Both systems have their positive and negative sides and are still being improved [75, 86].

1.5 Cell lines used in regenerative medicine

1.5.1 Mesenchymal stem cells

Research and clinical interest in MSCs has increased tremendously over the years, especially in the fields of tissue engineering and cellular therapies. The discovery of MSCs was first reported by Friedenstein et al. in numerous studies in the 1960s and 1970s [87]. Human mesenchymal stem cells (hMSCs) are multipotent progenitor cells, with the possibility of differentiation into various specialized cell types. The International Society for Cellular Therapy issued a position statement declaring a minimal criteria for cell characteristics and cell markers in 2006. The outlined characteristics were adherence to plastic, mesenchymal trilineage differentiation (osteogenic, chondrogenic and adipogenic), expandability over several passages, positive expression for CD73, CD 90, CD 105 and negative expression of CD14, CD19, CD34, CD45 and HLA-DR [88]. In tissue engineering, the differentiation potential of hMSCs in different cell types has attracted a certain amount of interest. Therefore, the utilization of hMSCs has become a key element in research for bone regeneration. Several *in vitro* and *in vivo* studies have been conducted concerning the use of hMSCs in BTE, although they remain challenging [89].

1.5.2 Umbilical vein endothelial cells

Human umbilical vein endothelial cells, also known as hUVECs, have been used in research for many years, mainly due to easy accessibility and availability. hUVECs are likely to be used when large quantities of cells are required. The first isolations and culturing of hUVECs were undertaken in the 1970s by Jaffe et al. [90]. hUVECs have a significant role in understanding the function and regulation of endothelial cells, as well as in angiogenesis and the interaction with other cell types. Especially in tissue engineering, hUVECs are the most frequently used types of endothelial cells for the vascularization of tissue. The properties of hUVECs have been analyzed over the years. The expression of endothelial markers and signaling molecules, as well as the possibility to differentiate into 3D models and to grow in co-culture make hUVECs extremely interesting for tissue engineering. Therefore, several studies on BTE have used hUVECs to enable prevascularized or vascularized scaffolds and some have already shown the development of functional vascular systems [91] [92].

1.6 Aim of the study

Critical-size-bone defects remain an urgent medical problem. Existing treatment options have not been considered ideal and the demand for other possibilities has been rising. BTE is a major research field, aiming to acquire further knowledge on optimal culture conditions, especially for osteogenesis and vascularization in osteoporotic patients. In the present study, we hypothesized that hMSCs, obtained from OFT (osteoporotic-fracture trauma) patients would behave differently in different oxygen concentrations, when compared to hMSCs from HET (high-energy trauma) patients. Therefore, culture conditions of 21% O₂, called normoxia, and 2% O₂, called hypoxia, were tested. As vascularization plays an important part in BTE as well, co-cultures with hUVECs were analyzed.

Main questions:

- Does oxygen level influence the proliferation and cell morphology of HET hMSCs differently than the OFT hMSCs?
- Does osteogenic differentiation potential in normoxia or hypoxia of HET hMSCs differ from the potential of OFT hMSCs?
- Is the osteogenic differentiation potential influenced in co-cultures with UVECs?
- Does the osteogenic differentiation potential of hMSCs in co-culture differ between the HET and OFT group?
- How does the co-culture influence the cell behaviour and morphology of UVECs?

2 Materials and Methods

2.1 Cell material

Cell material used in the experiments for this study was acquired with the consent of the patients and the Ethics Committee (238-15). For this work, all data were anonymous. Written approval and testing for HIV (human immunodeficiency virus) hepatitis B and hepatitis C was obtained prior to the bone marrow extraction.

Table 1: Cell material used in the experiment setup.

Donor Nr.	Origin/Firm	Age	DXA	Sex	Trauma
GFP expressing hUVECs	Pelobiotec GmbH	/	/	/	/
Nr.1	Iliac crest	43	/	Female	High-energy
Nr.2	Iliac crest	49	/	Female	High-energy
Nr.3	Iliac crest	30	/	Female	High-energy
Nr.4	Iliac crest	23	/	Female	High-energy
Nr.5	Proximal tibia	19	/	Female	High-energy
Nr.6	Proximal tibia	20	/	Female	High-energy
Nr.1	Femur head	94	-4,7	Female	Osteoporotic-fracture
Nr.2	Femur head	82	-2,6	Female	Osteoporotic-fracture
Nr.3	Femur head	70	-2,6	Female	Osteoporotic-fracture
Nr.4	Femur head	82	-3,6	Female	Osteoporotic-fracture
Nr.5	Femur head	85	-3,6	Female	Osteoporotic-fracture
Nr.6	Femur head	93	-3,6	Female	Osteoporotic-fracture

The high-energy trauma is referred to as HET and the mean donor age is 30.66 ± 12.62 years. The osteoporotic-fracture trauma is referred to as OFT and the mean donor age is 84.33 ± 8.77 years.

2.2 Isolation and expansion of donor cells

hMSCs were obtained from different bone donations. The bone marrow was scraped out by using a sharp spoon, washed with 30 ml phosphate buffered saline (PBS, Thermo Fisher, USA) and filtered through a 100 μ m sieve (cell suspension I). Subsequently, the hard bone pieces were incubated for 10 minutes in 10 ml of a 0.1% collagenase II (Collagenase 260 U/mg, Worthington Biochemical Corporation, USA) dispersed in PBS solution at 37°C under continuous agitation. The resulting cell suspension was again filtered through a 100 μ m sieve. This procedure was repeated three times to obtain 30 ml of suspension II. The resulting suspensions I and II were centrifuged. The resulting cell pellets were seeded with 10 ml of medium 1 in a T-75 cell culture flask (Nunc, Thermo Fischer, USA) and 1% fungicide (Patricin, Biochrom GmbH, Germany) was added. Cells were washed with PBS after three days, followed by a medium change. When the cell cultures reached confluence of 50-60%, they were trypsinized, counted and reseeded at a density of 2500 cells per cm^2 cell culture flask.

2.3 Cell counting

Cell counting was performed by using a Neubauer counting chamber. 10 μ l of cell suspension were added to the chamber and four large squares were counted.

The cell number was calculated using the following formula:

$$C = \frac{C_n 10^4 F}{4}$$

$$C_T = C \times C_s$$

C ... Cell density (cells/ml)

C_n ... Counted cell number

F ... Diluting Factor

C_T ... Total cell count

C_s ... Cell suspension volume

Trypan blue stain 0.4 percent (Invitrogen, Thermo Fischer, USA) was used as a live/dead stain by diluting the cell suspension at a ratio of 1:2 with the trypan blue solution. Living cells were not stained, while dead cells were stained blue due to their damaged cell membrane, enabling the diffusion of staining solution.

2.4 Thawing and cultivation of cells

After the cells were removed from a tank containing liquid nitrogen, they were thawed in a water bath at 37°C. Cells were cultured in a T225 cell culture flask prepared with 30ml preheated complete medium. hUVECs were cultured in endothelial cell growth medium (ECGM, Promocell, Germany) with supplement mix C-39125 (Promocell, Heidelberg, Germany). hMSCs were cultured in medium (referred to as medium 1) composed of minimum essential medium alpha-MEM (Gibco, Thermo Fischer, USA), 10% heat-inactivated fetal bovine serum (FBS, Sigma-Aldrich, USA) and 1% Penicillin/Streptomycin (P/S), at 10.000 U/ml / 10.000 µg/ml (Biochrom GmbH, Germany). Cells were cultured in either the normoxic (21% O₂) incubator (Memmert, Germany), or hypoxic (2% O₂) incubator (MCO-5M, Sanyo, Japan), with conditions at 37°C and 5% CO₂. The medium was changed twice a week. Additionally, cell adherence and confluence were controlled using a microscope (Axiovert 40 CFL, Zeiss, Germany).

2.5 Trypsinization and cryopreservation

Cells were passaged to prevent differentiation at a confluence of approximately 50-70%. Cells were washed twice with PBS to remove FBS and any cell suspension. Trypsinization was performed by using 1x trypsin (Trypsin/EDTA Solution 10x, Biochrom GmbH, Germany) in PBS. Trypsin was distributed equally in the whole cell culture flask and incubated at 37°C for 5-10 minutes. The reaction was inactivated with twice as much medium and the complete cell suspension was transferred to a tube. For hUVECs, inactivation was performed with 9-parts PBS and 1-part FBS in PBS (1:10). The cell culture flasks were seeded at a specific cell density of 5000 cells/cm². The following formula was used to calculate the cell suspension volume V_s :

$$V_s = \frac{C_T}{C}$$

V_s ... Cell suspension volume

C_T ... Target cell number

C ... Calculated Cell density (cells/ml)

The calculated cell volume was transferred into the cell culture flask and the remaining cell culture medium was added. The bottle was swiveled

well to spread the cells evenly. For cryopreservation of cell lines, the total cell count was determined and 1 million cells were frozen per cryovial. For this purpose, the cells were counted, centrifuged (500xg for 5 minutes) (Universal 16R, Hettich Zentrifugen, Germany) and resuspended in freezing medium (culture medium, 10% DMSO and 10% FBS). The cryovials were stored on dry ice and then placed in the nitrogen tank. In addition, microscopy images (Axiovert 40 CFL, Zeiss, Germany) were taken before freezing.

2.6 Cumulative population doubling and population doubling time

Analyzing the influence of normoxic and hypoxic cell culture conditions on cell proliferation, the cumulative doubling (cum PD), population doubling time (PDT) and area under the curve (AUC) were examined. Cumulative population doubling describes the total amount of times, cells in the population have doubled. 125.000 cells were seeded in a T25 bottle and counted after 4 or 6 days. Subsequently, 125.000 cells were transferred into a new cell culture flask until a decreasing cell number was observed.

Cumulative population doubling is calculated with the following formula:

$$CumPD = \frac{\ln(C_e/C_b)}{\ln 2}$$

C_e ... Cell number counted at the end

C_b ... Cell number counted in the beginning (n=125.000)

Population doubling time (PDT) is calculated with the following formula:

$$PDT = \frac{Time * \log(2)}{\log(C_e) - \log(C_b)}$$

PDT ... Population doubling time

t ... Time in days

C_e ... Cell number counted at the end

C_b ... Cell number counted in the beginning (n=125.000)

2.7 Morphological changes

Morphological changes of all 12 donors were imaged via phase contrast microscopy (Axiovert 40 CFL, Zeiss, Germany) until cells became senescent. Per donor, several pictures were taken and the cell area, circularity, ferret diameter and aspect ratio were examined for each culture condition using ImageJ analysis software [93]. Cells were manually encircled, paying attention to the fact that only single cells were counted. A minimum of 191 cells per donor, over different passages were evaluated.

2.8 Colony forming units and alkaline phosphatase activity

Colony-forming units (CFU) give an indication of cell proliferation capacity. In this study, colonies were stained with two different staining solutions, wherein one stained alkaline phosphatase activity (ALP), the other cells without ALP activity. ALP belongs to the group of known osteogenic markers [94]. For this experiment, 1.000 cells were placed in a 10 cm-culture

dish, ensuring their homogeneous distribution as individuals. Samples were cultured in normoxic and hypoxic conditions.

Cells were observed regularly and the medium was changed twice a week. After 11 days, a sufficient number of colonies were observed and it was still possible to distinguish one colony from another. In this assay, ALP-positive cells were stained dark purple with nitro-blue tetrazolium/5-bromo-4-chloro-3-indoly-phosphate (NTB/BCIP, Sigma-Aldrich, St.Louis, Missouri USA) and ALP-negative cells were stained pink with eosin (Eosin, Sigma-Aldrich, USA). Cells were washed with 4 ml of 1x PBS and fixed for 60 seconds with 4% PFA in 1x PBS. Samples were washed three times with buffer 1 for 5 minutes. Buffer 1 was composed of 100 mM trishydroxymethylaminomethane (Sigma-Aldrich, USA), 150 mM sodium chloride (NaCl, Carl Roth, Germany) and the pH adjusted to pH 7.5 with hydrochloric acid (HCl, Merck, Germany) and Aqua Dest. The cells were then covered in 1x NTMT (2x NTMT 1:1 with Aqua Dest.) twice for 5 minutes. 2x NTMT was composed of 5% 4M NaCl, 20% 1M TrisHCl (Sigma-Aldrich, USA), 10% 1M (MgCl₂, Carl Roth, Germany), 2% Tween-20 (Sigma-Aldrich, USA) and 63% distilled water (dH₂O). Finally, cells were stained for 15 minutes with the prepared staining solution, which contained 50% 2x NTMT, 50% polyvinyl alcohol (PVA, Sigma-Aldrich, USA) and 20µl/ml NBT/BCIP. Afterwards, cells were washed twice with aqua dest., stained with eosin for 12 minutes and washed with distilled water again. Colonies containing more than 50% ALP positive cells (dark purple) were designated as an ALP-expressing-colonies, while ALP negative cells were stained pink by the eosin (Sigma-Aldrich, USA). Samples were air-dried and photographed with the Leica M165 FC microscope and the colonies were counted. The efficiency of the CFU was determined using the following calculation equation:

$$E = \frac{N_e}{N_s} * 100\%$$

E ... Efficiency

N_e ... Number of counted colonies

N_s ... Number of seeded cells

2.9 Osteogenic differentiation

Cells were seeded at a density of 5000 cells/cm² and expanded. Monocultures with hMSCs were cultured in medium 1 (alpha-MEM, 10% FBS and 1% P/S). Co-cultures were cultured in endothelial cell growth medium 2 (ECGM2, Promocell, Germany) with supplement mix II C-39126 (Promocell, Germany). After reaching 80-90% confluence, osteogenic differentiation was induced by changing to the following medium: Dulbecco's modified eagle's medium (DMEM, Gibco, Thermo Fischer, USA), 10% FBS, 40 IU/ml P/S, 1 mM dexamethasone (Sigma-Aldrich, USA), 10 mM β-glycerophosphate (Sigma-Aldrich, USA), 50 µM L-ascorbic acid (Sigma-Aldrich, USA) and in co-cultures 10 ng/ml BMP-2 (Human BMP-2, MACS Miltenyi Biotec, Germany). Controls were seeded at the same density and received medium 1 without additives for osteogenic differentiation. Before reaching a confluence of 80-90%, cells were cultured in normoxic conditions. With the onset of osteogenic differentiation, cells for the hypoxia/normoxia experiment were cultured in normoxic and hypoxic conditions for 21 days. Co-culture experiments were kept in normoxic conditions for 14 days and medium was changed twice a week.

2.10 Alizarin Red staining and quantification

At the end of osteogenic differentiation (14 or 21 days), cells were washed twice with PBS and fixed with 4% paraformaldehyde (PFA, Merck, Germany) in PBS at room temperature. Subsequently, cells were washed twice with distilled water (Aqua Dest., Gibco, Thermo Fischer, USA) and stained with a 40 mM Alizarin Red staining solution (ARS). 40 mM ARS solution was prepared using Alizarin Red S (Alizarin Red S, Sigma-Aldrich, USA) dissolved in aqua dest and pH was adjusted to 4.1 with 0,5% ammonium hydroxide (Ammonium hydroxide solution, Sigma-Aldrich, USA). After 20 minutes of staining at room temperature, cells were washed with distilled water. This process was repeated until the water was clear. Samples were air dried and images were acquired with the Axio Observer Z1 (Zeiss, Germany) and Leica M165 FC (Leica, Germany) microscopes. The remaining staining solution was used to prepare a dilution series, varying from a concentration of 2 mM to 0.47 mM Alizarin Red. To obtain the different concentrations Alizarin Red was diluted with ammonium acetate (Sigma-Aldrich, USA). For the calculation of the standard curve, the optical density at 405 nm was measured using an ELISA reader (Multiskan FC, Thermo Fischer, USA). On the day of quantification, 0.5 ml of 10% acetic acid (Sigma-Aldrich, USA) was added to each well and incubated while being gently shaken for 30 minutes at room temperature. The cells were then softly scraped off the surface using a cell scraper and transferred to a 1.5 ml Safe Lock Eppi (Eppendorf Safe-Lock Tubes, Eppendorf, Germany). The acetic acid-cell mixture was vortexed for 30 seconds to ensure a homogeneous mixture, heated at 85°C (Thermomixer compact, Eppendorf, Germany) for 10 minutes, cooled on ice for 5 minutes and centrifuged at 14.000 x g for 15 minutes at room temperature. 375 µl of the supernatant was removed and transferred to a 2 ml reaction tube. The pH was adjusted between 4 and 4.5 by adding 150 µl of 3% ammonium hydroxide and monitoring using a pH indicator bar (pH indicator bar, Merck, Germany). The samples were transferred into triplicates in a 96-well plate and measured at 405 nm using an ELISA reader. The concentrations of all samples were calculated using the standard curve of known Alizarin Red concentrations.

2.11 3D seeding of a collagen scaffold with monocultures of hMSCs and co-cultures of hMSCs/hUVECs

A 3D approach to co-cultures was tested on a collagen scaffold. Osteogenic differentiation, cell survival and scaffold proprieties were examined. For this experiment, different hMSC donors, who also had OFT in their prehistory, were used.

The collagen scaffolds were seeded with a co-culture of donor hMSC and hUVECs, each at different ratios: 1:2 and 1:0. The scaffolds (Kollagen Re-sorb, Resorba Medical GmbH, Germany) were cut out with a biopsy punch (pfm medical ag, Cologne, Germany) the day before the experiment. The scaffolds were soaked in endothelial cell growth medium 2 (ECGM2, Promo Cell, Germany) for 24 hours. In addition, a 2% agarose solution (Biozym LE Agarose, Biozym Scientific, Germany) was prepared, and 300 µl of liquid agarose pipetted into each well of the 24-well plate, and dried. After drying, 1 ml of PBS was added to each well and the plates were sealed with parafilm and placed in the refrigerator overnight.

For the scaffold colonization, donor hMSCs and hUVECs were trypsinized and counted. To reach a cell density of 75.000 cells, the cell suspension was centrifuged down and resuspended at a specific volume of 667 µl of solu-

tion containing 50.000 cells. Different ratios were set up. At the ratio of 1:2, 667 μ l of hMSCs suspension was pipetted into a vial with 11334 μ l of hUVEC suspension. 2000 μ l of hMSC suspension at a ratio of 1:0 and 2000 μ l of the UVEC suspension at a ratio 0:1 were pipetted into a vial. Three scaffolds were added to the cell suspension and inoculated with the rotator (Multirotator PRT-35, Grant-bio, United Kingdom) in the incubator for three hours.

After 7 days, cell survival was checked using a life-death assay and the osteogenic differentiation was induced. The volume of the scaffold was regularly measured with ZEN lite 2012 (Version 1.1.2.0, Zeiss, Germany)

2.12 Determination of cell survival using life-death-assay

Fluorescence-based life/death measurements are used to determine cell survival. Simultaneous staining was undertaken with two dyes, whereby one stained the living cells (green) and the other marked the dead cells (red). Fluorescein diacetate (FDA, Thermo Fischer, USA) is collected by living cells and converted into the fluorescent metabolite fluorescein (green). In contrast, the nuclear staining is performed using propidium iodide (PI, Sigma-Aldrich, USA), which is only permeable through the membrane of dead cells. In this study, stock solutions were prepared for both stains. For the fluorescein diacetate stock solution, 5 mg of FDA were dissolved in 1 ml of acetone and stored at -20°C. For the propidium iodine stock solution, 2 ml of PI were dissolved in 1 ml of PBS and stored at 4°C. On the day of staining, the following staining solution was prepared: culture medium (5ml), 5mg/ml FDA, 2mg/ml PI.

2.13 Statistical analysis

Two major experiments were performed, the hypoxia/normoxia experiment, referred to as experiment I, and the hUVECs/hMSCs co-culture experiment, referred to as experiment II. All experiments were performed with the isolated hMSCs from the above mentioned twelve donors, six from the HET group and six from the OFT group.

Table 2: Experiment 1 set up

Experiment	Multiplications	Statistical Test
Analysis of morphology changes Colony forming units Osteogenic differentiation	Triplet Duplicate Triplet	One way Anova

Table 3: Experiment 2 Set up

Experiment	Multiplications	Statistical test
Osteogenic differentiation Survival of hUVECs in co-cultures	Duplicate Duplicate	One way Anova

Statistical analysis was performed using Graphpad Prism 9 (Version 9.1.0, Graphpad Software Inc., USA) and RStudio (RStudio Inc., Boston, Massachusetts, USA). Results were illustrated as mean \pm SD and median (+) or graphically as box, bar or whisker plot. For statistical analysis between two groups, Student's t-test for equal variances or the Welch test for unequal

variances were performed. If no Gaussian distribution was given, a Mann-Whitney test was performed. Comparison between more than two groups was performed with one-way Anova if a Gaussian distribution was given, if not a Kruskal-Wallis test was performed. Values of $p < 0.05$ were considered significant.

3 Results

3.1 Hypoxia maintains cell morphology and proliferation over time

3.1.1 Cell morphology

Cell morphology is an important factor in the context of analyzing behaviour and changes in a cell culture. Changes in morphology can be an indicator of cellular senescence whereas in general, cells become large, flat, vacuolized and, occasionally, multinucleated [52].

Cell morphology was analyzed in both the normoxia and hypoxia culture conditions, for all 12 donor samples over the entire period of the cumulative population doubling experiment. For most donor samples, this period was 31 days, exceptions saw cells proliferated for only 20 or 25 days (HET: D.3, D.4 and D.6, OFT: D.1, D.2, D.3 and D.5). Figure 2 shows a qualitative overview of two donor samples, with one from each group (A: HET D.5, B: OFT D.4). In the first days cells had a spindle shaped figure in hypoxia and normoxia in both the HET and OFT groups. With every trypsinization, the cells became slightly more flattened in both the normoxia and hypoxia situations and both groups (HET OFT). Macroscopically, there were no significant differences in cell morphology when comparing normoxia and hypoxia, nor when comparing the HET group to OFT group.

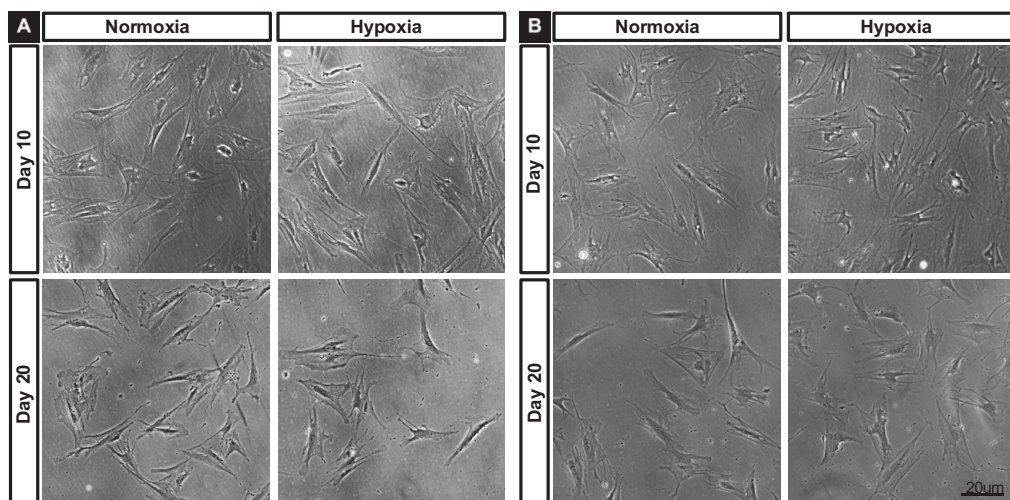


Figure 2: Exemplary microscopy of the morphological changes in hMSCs from the HET (A) and OFT (B) group in normoxia and hypoxia after 10 and 20 days. Macroscopically, there were no significant differences in cell morphology, neither comparing normoxia to hypoxia, nor when comparing the HET group to the OFT group. A. HET donor 5 B. OFT donor 4, Bar equals 20 μ m

The quantification of morphological parameters in normoxic compared to hypoxic cell culture conditions is shown in Figure 3.

On day 10, the mean area for the HET group in normoxia was $10,151.09 \pm 4,846.85 \mu\text{m}^2$ and in hypoxia the mean area was $7,688.67 \pm 4,145.52 \mu\text{m}^2$. For the OFT group, the mean area was $7,589.78 \pm 4,052.64 \mu\text{m}^2$ in normoxia and $7,814.11 \pm 4,319.92 \mu\text{m}^2$ in hypoxia. On day 10, calculations showed a significant change comparing the area in normoxia to hypoxia for the HET group and a non-significant change for the OFT group (HET: $p < 0.0001$, OFT: $p > 0.999$). In hypoxic cell culture conditions cells showed a tendency towards a smaller area. Cells in normoxic conditions showed a tendency towards

flattening. Comparing the HET group to the OFT group, a significant change was observed in normoxia, where the area of HET cells was significantly larger, but the difference was not seen in hypoxia (normoxia: $p<0.0001$, hypoxia: $p>0.999$)

On day 20, the mean area for the HET group in normoxia was $8,917.07 \pm 5,388.83\mu\text{m}$ and in hypoxia the mean area was $7,353.94 \pm 4,229.28\mu\text{m}$. For the OFT group, the mean area in normoxia was $8,286.23 \pm 4,274.55\mu\text{m}$ and $7,465.57 \pm 4,168.09\mu\text{m}$ in hypoxia. On day 20, cells cultured in normoxia showed a more pronounced flattening, whereas cells in hypoxia kept a smaller area. The change was significant for the HET group, but not for the OFT group (HET: $p=0.0002$, OFT: $p=0.0762$). Analysis of the area measurements between both groups (HET to OFT) showed no significant change in normoxia or hypoxia (normoxia $p>0.999$, hypoxia $p>0.999$).

Comparison of the area measurements between days 10 and 20 for the HET group cultured in normoxia showed a significant change, where the area measured on day 10 was bigger than day 20 ($p=0.0012$). For the HET group in hypoxia no significant change was seen ($p>0.999$). Comparing the area measurements on day 10 to day 20 no significant change was seen for the OFT group (normoxia $p>0.999$, hypoxia $p>0.999$).

In regard to the aspect ratio, no significant change could be seen when comparing hypoxia to normoxia, or HET to OFT. The only significant change was calculated when comparing the aspect ratio of the HET group from day 10 to day 20 ($p=0.0092$). For the OFT group, no significant change was shown. As only a small number of donor samples continued growing until day 31, statistical analyses were performed on day 10 and 20.

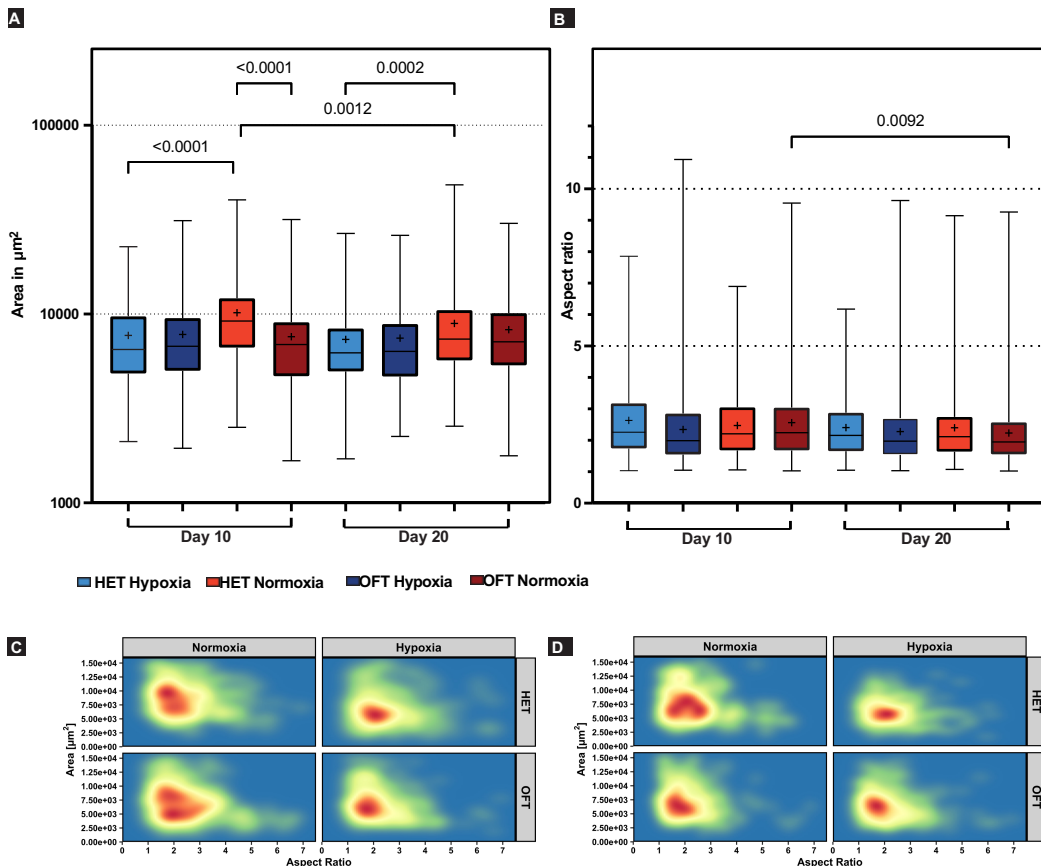


Figure 3: A and C: Quantification of cell area in normoxia and hypoxia for all HET and OFT groups. Day 10 (A): Comparing hypoxic to normoxic cell culture conditions, a significant change in area was observed for the HET group ($p<0.0001$) and a non-significant change for the OFT group ($p>0.999$). Comparing the HET to the OFT group in normoxia, a significant change was observed, but a non-significant difference was observed in hypoxia (normoxia $p<0.0001$, hypoxia $p>0.999$). Day 20 (B): Comparing hypoxia to normoxia for the HET group, the change was significant (HET $p=0.0002$). For the OFT group, the change was not significant ($p=0.0762$). Comparing HET to the OFT group, a significant change was not seen in either normoxia or hypoxia (normoxia $p>0.999$, hypoxia $p>0.999$). Comparison of the area measurements on day 10 and day 20 for the HET group cultured in normoxia, showed a significant change ($p=0.0012$). In hypoxia, no significant change was seen ($p>0.999$). Comparing the area measurements on day 10 to day 20, no significant change was seen for the OFT group (normoxia $p>0.999$, hypoxia $p>0.999$). B and D: Quantification of the aspect ratio in normoxia and hypoxia on day 10 and day 20, for both the HET and OFT groups. Comparing hypoxia to normoxia, no significant change was calculated for the HET or OFT groups. Only comparison of day 10 to day 20 for the OFT group in normoxia showed a significant change ($p=0.0092$). Box and whisker plot (min and max point), with median (line) and mean (+). Only significant changes are represented graphically.

To conclude, cell morphology was influenced by oxygen concentrations and cell flattening occurred at a later stage in the hypoxic environment than in the normoxic environment.

3.1.2 Cumulative population doubling

Several studies have shown that hypoxic cell culture conditions have positive effects on cell proliferation [44]. CumPD was calculated to investigate if these conditions would also influence the proliferation capacity of the HET group and of the OFT group. Figure 4 shows the cumPD of the different donors in both groups (A: HET, B: OFT).

Most donor cells showed a similar behaviour concerning their cumPD. The normoxic and hypoxic cell culture conditions had no influence on the cumPD until day 5. After 5 days, most donors showed a higher proliferation in hypoxia compared to normoxia, where proliferation decreased.

For the HET group (Figure 4 part A), three out of six donor samples continued growing in both oxygen levels until day 31, although hypoxic conditions were superior to normoxic conditions. The cells of HET D.3 ceased growth on day 25 in normoxia and kept growing in hypoxia. Regardless of oxygen levels, the cells of HET D.4 ceased growth on day 20. The cells of HET D.6. ceased growth on day 20 in hypoxia; in normoxia they continued their growth process until day 25.

For the OFT group (Figure 4 part B) several donor samples showed continued growth in hypoxia until day 31 (OFT D.3, D.4, D.6). OFT D.1 stopped growing on day 20 under both conditions. OFT D.2 and D.5 showed shortened growing in normoxic compared to hypoxic cell culture conditions.

After cells ceased growth, which manifested as decreasing or stagnated proliferation, the experiments were stopped.

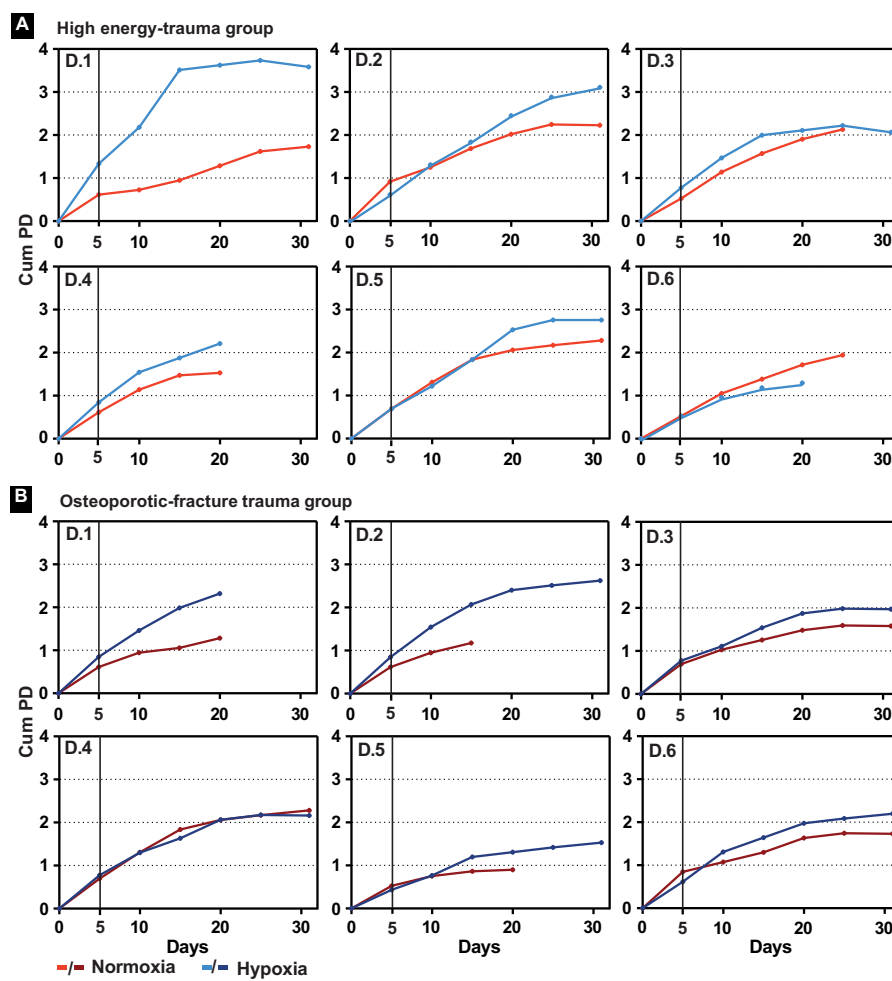


Figure 4: CumPD of all donors in the HET group (A) and OFT group (B) in normoxic and hypoxic cell culture conditions. For almost all donors (except HET D.6 and OFT D.4) proliferation was higher in hypoxic cell culture conditions. For most donors in the HET and the OFT groups, proliferation was similar until day 5. After 5 days, proliferation in hypoxic cell culture conditions continued, whereas proliferation reduced in normoxic culture conditions. This effect was noted especially for donor D.1 in the HET group, where proliferation almost doubled in hypoxic cell culture conditions. For all the other donors in the HET group, except D.6, proliferation was improved in hypoxic cell culture conditions. A similar effect was seen for the OFT group. For several donor samples (D.2 and D.5) in the OFT group, cells ceased growth in normoxic conditions, whereas they kept growing in hypoxic conditions. Comparing the proliferation capacity of the HET to the OFT group, a slightly higher proliferation capacity was observed for the HET group.

Figure 5 illustrates the behaviour of the HET and OFT group in normoxic and hypoxic cell cultures. HET donor samples reached a mean cumPD of 1.75 ± 0.30 in normoxia and a mean cumPD of 2.37 ± 0.75 in hypoxia ($p=0.174$). On day 20, a mean cumPD of 1.39 ± 0.42 was calculated for the OFT group in normoxic conditions and a mean of 1.99 ± 0.39 was calculated in hypoxic ($p=0.199$). Under both conditions, although HET donor samples performed better than OFT donor samples, the results were non-significant (normoxia: $p=0.612$, hypoxia $p=0.565$). The only significant change was seen when comparing the HET group in hypoxia to the OFT group in normoxia ($p=0.014$). To ascertain the cumPD in relation to the donor age, another graph was created and is provided in the supplementary data, figure 15

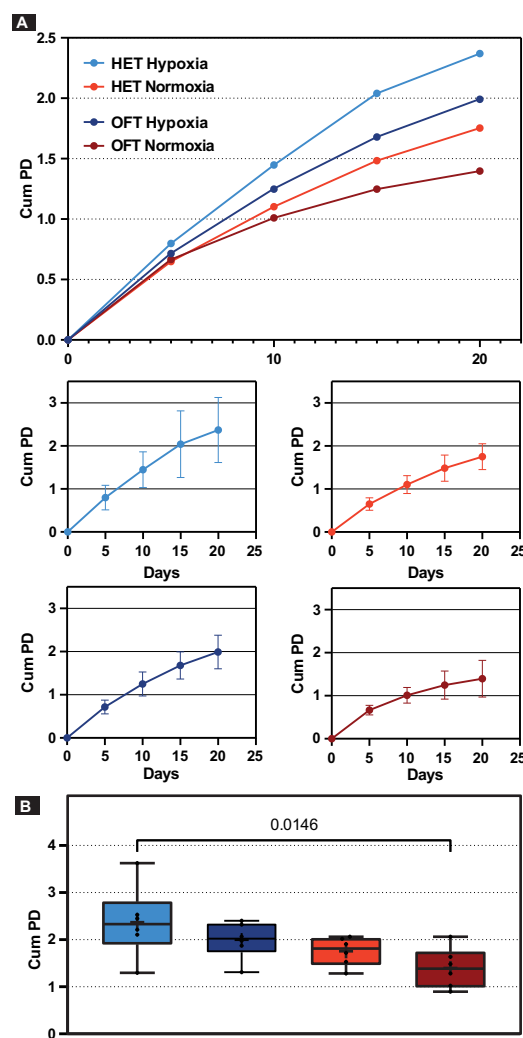


Figure 5: A: CumPD comparison between the HET group and the OFT group in normoxic and hypoxic cell culture conditions over a period of 20 days. HET donor samples reached a mean cumPD of 1.75 ± 0.30 in normoxia and a mean cumPD of 2.37 ± 0.75 in hypoxia. ($p=0.174$). For the OFT group, there was a mean cumPD of 1.39 ± 0.42 in normoxic conditions and a mean cumPD of 1.99 ± 0.39 in hypoxic conditions ($p=0.199$). B: CumPD pooled in the HET and OFT groups and comparison of normoxia to hypoxia. Under both conditions, although HET donor samples performed better than OFT donor samples, the results were non-significant (normoxia: $p=0.612$, hypoxia $p=0.565$). The only significant change was seen when comparing the HET group in hypoxia to the OFT group in normoxia ($p=0.014$). Graph: Box and whisker plot (min and max point) with median (line) and mean (+). Only significant changes are represented graphically.

The AUC was calculated by using figure 4, enabling comparison between both conditions and both groups (Figure 6). AUC was only calculated up to day 20, as cumPD values could not be obtained for all donors on day 25 or

31.

Examining the proliferation capacity of each donor sample individually (Figure 6 A), most donors showed higher proliferation capacity in hypoxia compared to normoxia. Only a few donor samples (HET D.6 and OFT D.4) showed greater growth potential in normoxia.

Randomizing the groups into HET and OFT groups as shown in (Figure 6 B), the mean AUC values for the HET donor samples were 20.56 ± 3.63 in normoxia and 27.36 ± 9.08 in hypoxia ($p=0.135$). OFT donor samples showed a mean AUC of 18.11 ± 3.93 in normoxia and 23.19 ± 4.66 in hypoxia ($p=0.0681$). Both groups (HET and OFT) showed a tendency towards a higher proliferation capacity in hypoxia. Comparing the HET group to the OFT group, no significant difference was found in normoxic or hypoxic cell culture conditions (normoxia $p=0.2876$, hypoxia: $p=0.3478$). Only a trend towards a better performance in the HET group group, could be determined.

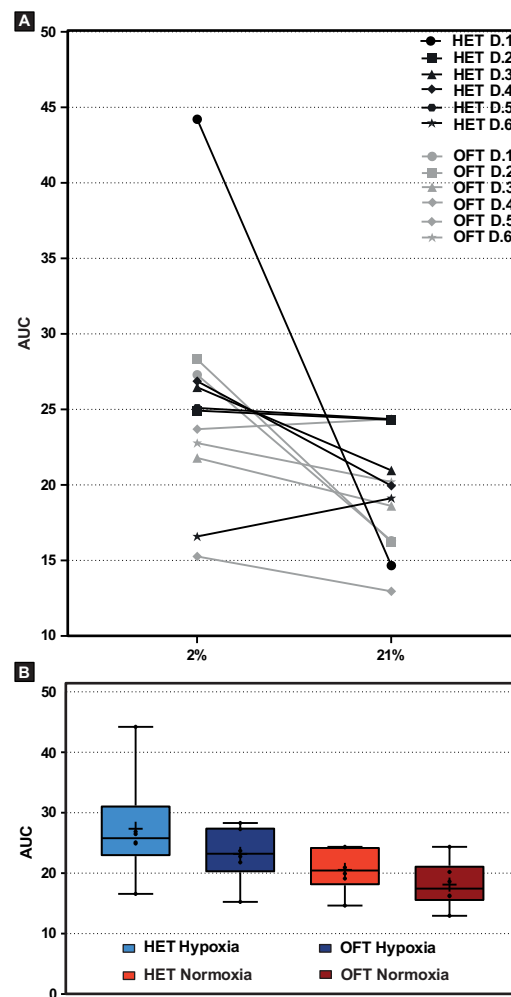


Figure 6: A: Each donor sample in the HET and OFT groups is presented individually. The AUC in shown for both culture conditions (normoxia and hypoxia). In particular, donor 1 in the HET group displayed a considerable difference between normoxia and hypoxia, showing a higher AUC in hypoxia. On the other hand, donor 6 in the HET group showed a slight decrease in hypoxia. For the OFT group, with the exception of donor 4, all donors showed a better growth potential in hypoxic cell culture conditions. B: AUC comparing HET and OFT groups in normoxic and hypoxic cell culture conditions after 20 days of cell culture. Significant changes were not found in the HET or in the OFT group, when comparing the AUC in hypoxic to normoxic cell culture conditions (HET $p=0.135$, OFT $p=0.0681$). However there was a tendency towards higher proliferation capacity in hypoxia. When comparing the groups (HET to OFT), no significant changes were observed (normoxia: $p=0.2876$, hypoxia: $p=0.3478$). Graph: Box and whisker plot (min and max point) with median (line) and mean (+). Only significant changes are represented graphically.

To conclude, cells in normoxic cell culture conditions entered the stationary phase earlier than cells in hypoxic conditions.

3.1.3 Colony forming units

CFU estimate the ability to establish colonies under specific conditions, in this case those conditions were normoxia and hypoxia. Figure 7 shows an overview of the CFU of all 12 donor samples under both conditions and their efficiency. The HET group showed a mean CFU of 38.16 ± 22.21 units in normoxia, compared to a mean CFU of 68.6 ± 17.85 units in hypoxia ($p=0.221$). The OFT group showed a mean CFU of 36.75 ± 31.58 units in normoxic conditions and 58.16 ± 31.40 units in hypoxic conditions ($p=0.502$). Both groups, HET and OFT, showed a trend towards a higher CFU number in hypoxia compared to normoxia. Comparing the HET group to the OFT group, a non-significant change was observed (normoxia: $p=0.999$, hypoxia: $p=0.900$). However there was a tendency towards a better performance in the HET group. To ascertain the CFU in relation to the donor age, another graph was created and is provided in the supplementary data, figure 15

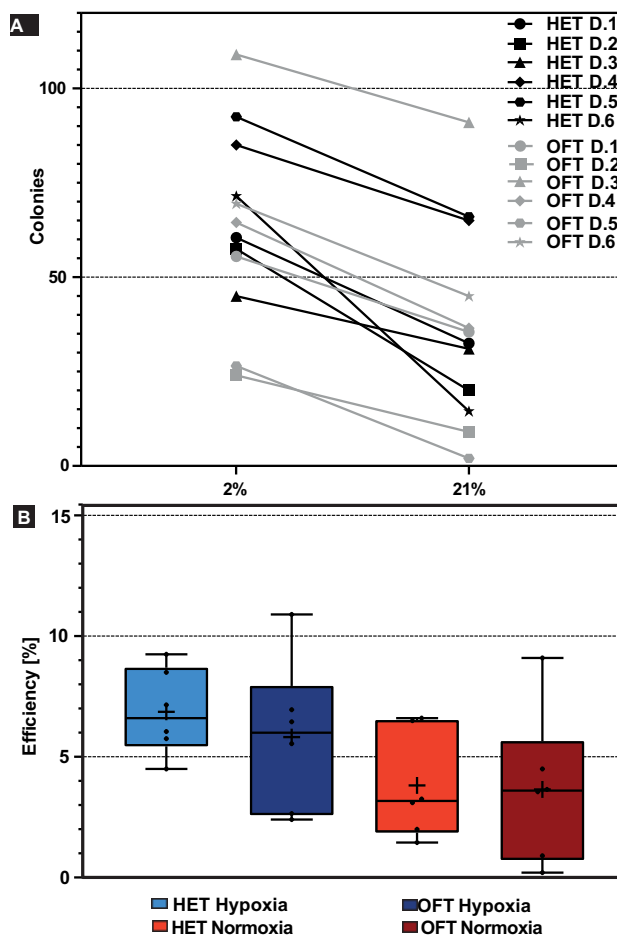


Figure 7: CFU (A) and efficiency (B) of the HET and OFT groups in hypoxia and normoxia. A: The HET and the OFT group show a higher number of colonies in hypoxic cell culture conditions. B: As for the efficiency, the HET group revealed a non-significant change when comparing the two culture conditions (normoxia/hypoxia) ($p=0.221$), as did the OFT group ($p=0.502$). Comparing the HET to the OFT group, a non-significant change was observed (normoxia: $p=0.999$, hypoxia: $p=0.900$). Graph: Box and whisker plot (min and max point) with median (line) and mean (+). Only significant changes are represented graphically.

3.2 Osteogenic differentiation potential of the HET group and OFT group in normoxia and hypoxia

Varied conditions can influence the osteogenic differentiation potential of hMSCs positively or negatively. Osteogenic differentiation was induced for 21 days and ARS was performed to quantify the osteogenic differentiation potential (Figure 8). Most donor cells, regardless of the conditions, were able to induce mineralization by forming a more or less homogeneous matrix. Macroscopically, it appeared as if the matrixes produced by the HET donors (A) were more developed when compared to the OFT donors matrixes (B). Moreover, mineralization seemed stronger in normoxic conditions than in hypoxic conditions. Neither control group (HET and OFT control groups not induced to osteogenic differentiation) produced a calcified matrix.

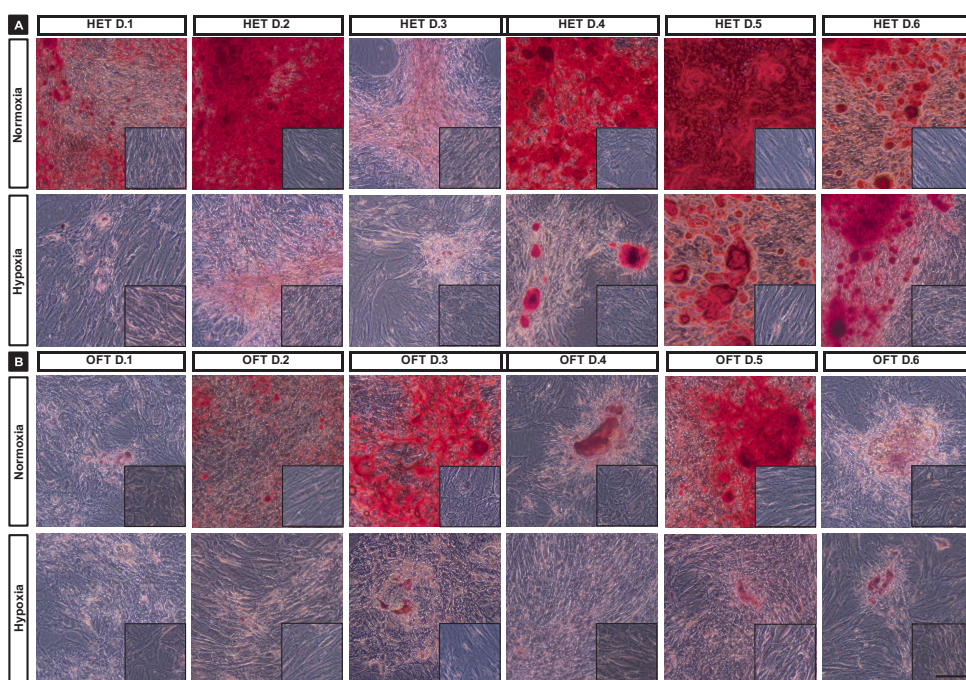


Figure 8: Exemplary microscopy images of osteogenic differentiation and ARS in the HET group and OFT group. The images in the right corners represent the corresponding controls (not induced to osteogenic differentiation). All hMSCs were cultured in normoxia and hypoxia. Microscopically almost all donors in the HET group show a homogeneous matrix and staining in normoxia. Only D.3 showed a weaker staining signal. In hypoxia, they showed less mineralization. Macroscopically the OFT group showed less mineralization in hypoxic conditions than in normoxic cell culture conditions. Comparing the HET group to the OFT group, especially in normoxia, the staining signal seemed stronger for the HET group. Only a slight difference (HET/OFT) was noticeable in hypoxia. Bar equals 20 μ m

The osteogenic differentiation potential was evaluated by quantifying the ARS of all donors (Figure 9 A). The osteogenic differentiation potential covered a large range of values for all donors, varying from ARS concentrations of 9.69 ± 0.5 mM (HET D.5) to 0.06 ± 0.038 mM (OFT D.6) in normoxic conditions and ARS concentrations of 1.20 ± 1.16 mM (HET D.5) to 0.025 ± 0.011 mM (OFT D.2) in hypoxic conditions. For most donors, the calculated ARS concentration was higher in normoxia than in hypoxia. Only a few donors showed (e.g. HET D.6 and OFT D.6) a similar or lower ARS concentration in normoxia.

The behaviour of the HET group and OFT groups during osteogenic differentiation was evaluated (Figure 9 B). For the HET group, the results was a mean AR concentration of 2.544 ± 3.808 mM in normoxia and a mean AR of 0.305 ± 0.448 mM in hypoxia. In both conditions, control groups pro-

duced ARS concentration close to zero (normoxia: $0.0031 \pm 0.017\text{mM}$, hypoxia: $0.041 \pm 0.016\text{mM}$). Comparing the osteogenic differentiated HET group to the control group, a significant change was calculated in normoxia ($p=0.005$). However, in hypoxia, osteogenic differentiation was not significantly different, compared to the control group ($p=0.998$). The comparison of the osteogenic-induced HET group in normoxia to the same in hypoxia revealed a non-significant change ($p=0.057$).

The OFT group presented a mean ARS concentration of $0.189 \pm 0.194\text{mM}$ in normoxic cell cultures. The average ARS concentration in hypoxic conditions was $0.046 \pm 0.014\text{mM}$. ARS concentration showed a non-significant change when comparing the osteogenic differentiated OFT group in normoxia or hypoxia to the control group (normoxia $p=0.999$, hypoxia $p=0.999$). No significant changes were observed when comparing the induced OFT group in normoxic and hypoxic conditions ($p>0.999$).

A significant change was observed when comparing the HET group to the OFT group in normoxia ($p=0.039$), but no significant change was observed when comparing both groups in hypoxia ($p=0.999$). Additionally, a significant change was observed when comparing the osteogenic differentiated OFT group in hypoxia to the osteogenic differentiated HET group in normoxia ($p=0.024$). Normoxic cell culture conditions and the HET group demonstrated a tendency towards an increased osteogenic differentiation.

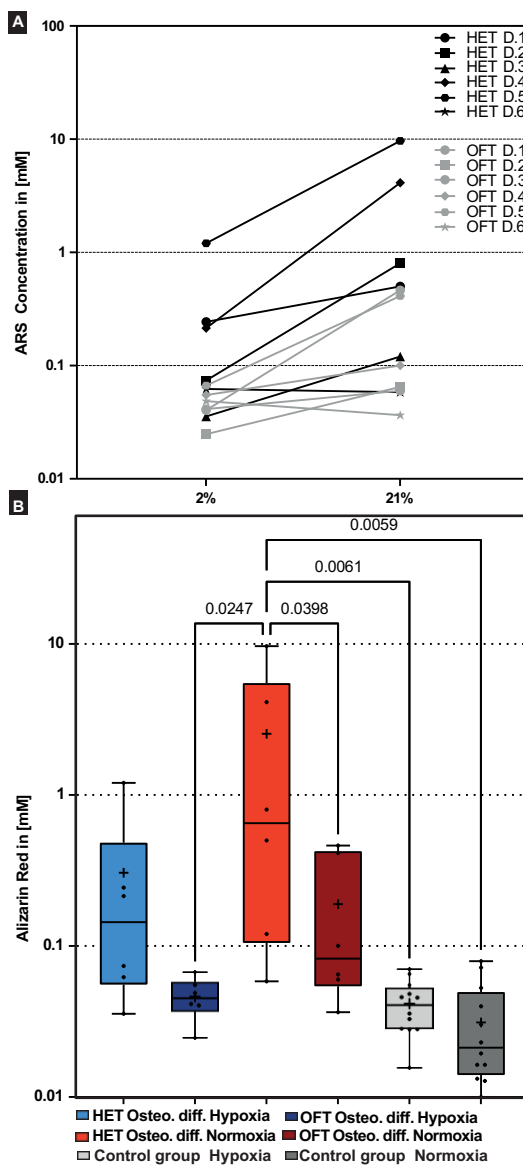


Figure 9: A: Alizarin Red quantification of all hMSCs donors in normoxic and hypoxic cell cultures. Except for HET D.6 and OFT D.6 which showed a decrease of the ARS concentration, all donors displayed a tendency towards a better osteogenic differentiation in normoxic cell culture conditions. B: Alizarin Red staining quantification of the HET and OFT groups in normoxic and hypoxic cell culture conditions and in the associated control group. The HET group showed a mean ARS concentration of 2.544 ± 3.808 mM in normoxia and 0.305 ± 0.448 mM in hypoxia. The OFT group presented a mean ARS concentration of 0.189 ± 0.194 mM in normoxia and an average ARS concentration of 0.046 ± 0.014 mM in hypoxia. In both conditions, control groups produced ARS concentration close to zero (normoxia: 0.0031 ± 0.017 mM, hypoxia: 0.041 ± 0.016 mM). Comparing the osteogenic differentiated group to the control group, a significant change was observed in normoxia for the HET group ($p=0.005$). For the OFT group, the change was not significant ($p=0.999$). A non-significant ARS concentration was calculated when comparing the osteogenic differentiation group to the control group in hypoxia (HET: $p=0.998$; OFT $p=0.990$). Comparing HET to the OFT group in normoxia there was a significant difference ($p=0.039$), but the difference was not significant in hypoxia ($p=0.999$). Graph: A: Individual values paired in normoxia and hypoxia. B: Box and whisker plot (min and max point) with median (line) and mean (+). Only significant changes are represented graphically.

Figure 10 A shows that most donor cells from both groups had increased osteogenic differentiation in normoxia compared to hypoxia. Osteogenic differentiation in hypoxia, ranging above n-fold of 10 (e.g. n-fold=11.5 for OFT D.3, n-fold=10.9 for HET D.2, n-fold=19.2 in HET D.4). Only two donor samples, one from each group showed a decreased mineralization: HET D.6 and OFT D.6. In 10 B, donor samples were pooled in the two major groups, HET and OFT, with a non-significant change observed ($p=0.334$). However, the HET group showed a tendency towards a better osteogenic differentiation compared to the OFT group.

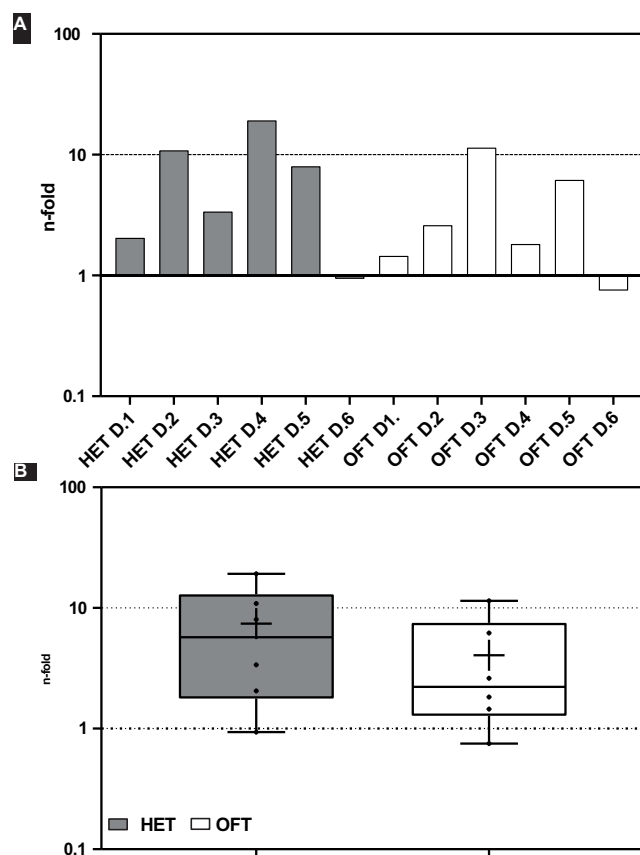


Figure 10: Increase or decrease of the different donor samples in normoxic compared to hypoxic cell cultures. A. All donors, except HET D.6 and OFT D.6, showed an increased mineralization in normoxic cell culture conditions. B. Comparison the two major groups HET and OFT ($p=0.334$). Graph: Bar plot (A) and box plot (B) with min. and max. point, median (line) and mean (+). Only significant changes are represented graphically.

3.3 Co-culture of hMSCs and hUVECs enhance osteogenic differentiation capacity

As mentioned in the previous chapter, different conditions can influence the osteogenic differentiation potential. In this experiment, the influence of a co-culture with hUVECs was evaluated. The co-cultures were seeded at different ratios (hMSCs:hUVECs), 1:0, 1:2 and 1:3 and differentiated for 14 days, after which ARS was performed.

Macroscopically, almost all donor cells, at all ratios, showed the potential to differentiate and forming a more or less homogeneous extracellular matrix. It seemed that the ARS signal for the co-cultured cells (hMSCs:hUVECs, 1:2 and 1:3) was stronger than for the single cultured hMSCs (Figure 11). Control groups displayed no mineralization. Several induced cell cultures, mostly co-cultures, showed holes in the cell layers. Microscopic

images in higher resolution provided as supplementary data figure 16 show that the holes are not filled with cells.

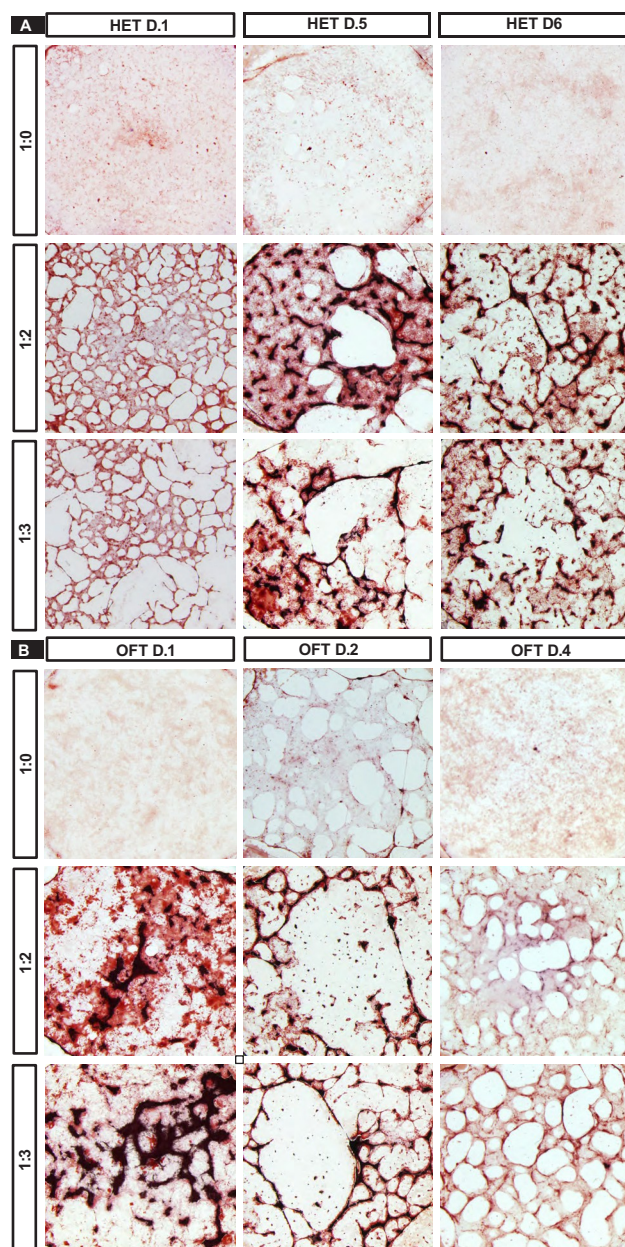


Figure 11: Exemplary microscopy images of ARS of HET donor samples (A) and OFT donor samples (B) at different ratios with hUVECs during osteogenic differentiation. Macroscopically, mineralization was produced in all three ratios (hMSCs:hUVECs). Increased mineralization was observed for co-cultures (hMSCs:hUVECs) in ratios of 1:2 and 1:3. Bar equals 1000 μ m

The osteogenic differentiation potential was quantified using ARS. The donor samples showed clear variances in their osteogenetic differentiation potential (Figure 12). At all three ratios, control groups (not induced to osteogenic differentiation), produced ARS signals close to zero (1:0: 0.016 ± 0.024 mM, 1:2: 0.011 ± 0.011 mM and 1:3: 0.007 ± 0.003 mM).

In the HET group, ARS concentration values ranged from 0.540 ± 0.260 mM (HET D.1 at ratio 1:2) to 0.006 ± 0.006 mM (HET D.4 at ratio 1:2). HET monocultures a mean ARS concentration of 0.230 ± 0.130 mM was calculated. HET co-cultures a mean ARS concentration of 0.300 ± 0.232 mM at a ratio of 1:2 and a mean AR of 0.256 ± 0.144 mM at a ratio of 1:3 was calculated. Comparing the osteogenic differentiated HET group to the control

group (not induced to osteogenic differentiation), all three ratios showed a significant difference (1:0: $p=0.0192$, 1:2: $p=0.0005$ 1:3: $p=0.0047$). Comparison of the osteogenic differentiation potential of the different found there was no significant difference in either the HET 1:0 to the 1:2 ($p=0.985$), the HET 1:0 to 1:3 ($p>0.999$), nor the HET 1:2 to the 1:3 group comparison ($p=0.999$).

In the OFT group, ARS concentrations varied from 0.533 ± 0.019 mM (OFT D.2 at ratio 1:2) to 0.003 ± 0.003 mM (OFT D.5 at ratio 1:3). OFT monocultures a mean ARS concentration of 0.146 ± 0.138 mM was calculated. OFT group co-cultures a mean ARS concentration of 0.256 ± 0.216 mM at a ratio of 1:2 and a mean ARS concentration of 0.255 ± 0.178 mM at a ratio of 1:3 was calculated. Comparison of the osteogenic differentiated OFT group to the control group showed a difference (1:0: $p=0.420$, 1:2: $p=0.0051$, 1:3: $p=0.0048$). ARS concentration was not significantly different when comparing the osteogenic differentiated OFT 1:0 to the 1:2 ($p=0.829$), the 1:0 to 1:3 ($p=0.832$), nor the 1:2 to 1:3 group ($p>0.999$).

When comparing the HET to the OFT group, there was not a significant difference in osteogenic differentiation potential at the ratio of 1:0 ($p=0.3939$), nor at the ratio of 1:2 ($p=0.7399$) or at the ratio of 1:3 ($p=0.9969$). A wide scattering of the different ARS concentrations of the donors was observed.

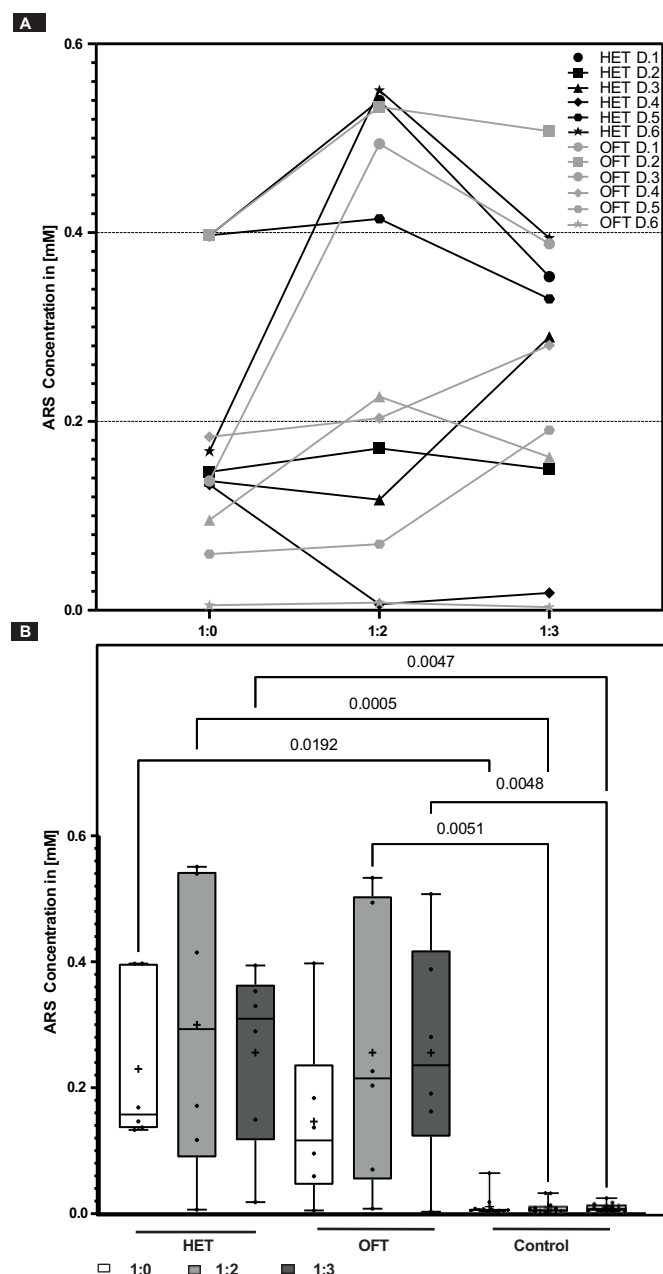


Figure 12: A: ARS quantification of all donor samples in monocultures and co-culture with hUVECs in different ratios undergoing osteogenic differentiation. For most donor samples, in both the HET and the OFT group, co-cultures enhanced the mineralization process. For several donors this enhancement was especially notable in the 1:2 ratio, (e.g. HET D.1, HET D.6 and OFT D.1, OFT D.2, OFT D.3). However, HET D.4 showed decreased mineralization in both ratios. B: HET donor monocultures a mean ARS concentration of 0.230 ± 0.130 mM was calculated. HET donor co-cultures a mean ARS concentration of 0.300 ± 0.232 mM at a ratio of 1:2 and a mean ARS concentration of 0.256 ± 0.144 mM at a ratio of 1:3 was calculated. At all three ratios, ARS concentration calculated for the control groups were close to zero (1:0: 0.016 ± 0.024 mM, 1:2: 0.011 ± 0.011 mM, 1:3: 0.007 ± 0.003 mM). Comparison of the HET osteogenic differentiated group to the HET control group showed a significant difference for all three ratios (1:0: $p=0.0094$, 1:2: $p=0.0152$ 1:3: $p=0.0022$). Comparison of the osteogenic differentiation ARS concentrations showed no significant difference in neither the HET 1:0 to the 1:2 ($p=0.985$), the HET 1:0 to 1:3 ($p>0.999$), nor the HET 1:2 to the 1:3 group ($p=0.999$). OFT group monocultures a mean AR of 0.146 ± 0.138 mM was calculated. OFT group co-cultures a mean AR of 0.256 ± 0.216 mM at a ratio of 1:2 and a mean AR of 0.255 ± 0.178 mM at a ratio of 1:3 was calculated. Comparison of the ARS concentration of the osteogenic differentiated OFT group to the control group a difference was shown (1:0: $p=0.420$, 1:2: $p=0.0051$, 1:3: $p=0.0048$). ARS concentration was not significantly different when comparing the OFT 1:0 to the 1:2 ($p=0.829$), the 1:0 to 1:3 ($p=0.832$), or the 1:2 to 1:3 group ($p>0.999$). When comparing the HET to the OFT group, there was no significant difference ($p=0.393$) in osteogenic differentiation potential at the ratio of 1:0, the ratio of 1:2 ($p=0.7399$) or at the ratio of 1:3 ($p=0.9969$). A wide scattering of the different ARS concentrations of the donors is observed. Graph A: Individual values connected by line at different ratios B: Box and whisker plot (min and max point) with median (line) and mean (+). Only significant changes are represented graphically.

The HET group showed that osteogenic differentiation potential was positively influenced in co-cultures for several donor samples (HET D.3 and D.6) (Figure 13). However, some donor samples (HET D.4 and D.5) showed a lowered or unaltered potential. The OFT group was positively influenced by co-cultures for all donor samples, except one (OFT D.5 at ratio 1:3). As Figure 13 B illustrates, OFT donors had a stronger tendency for differentiation than HET donors, leading to a better osteogenic differentiation potential in co-cultures ($p=0.362$ at ratio 1:2 HET/OFT, $p=0.254$ at ratio 1:3 HET/OFT).

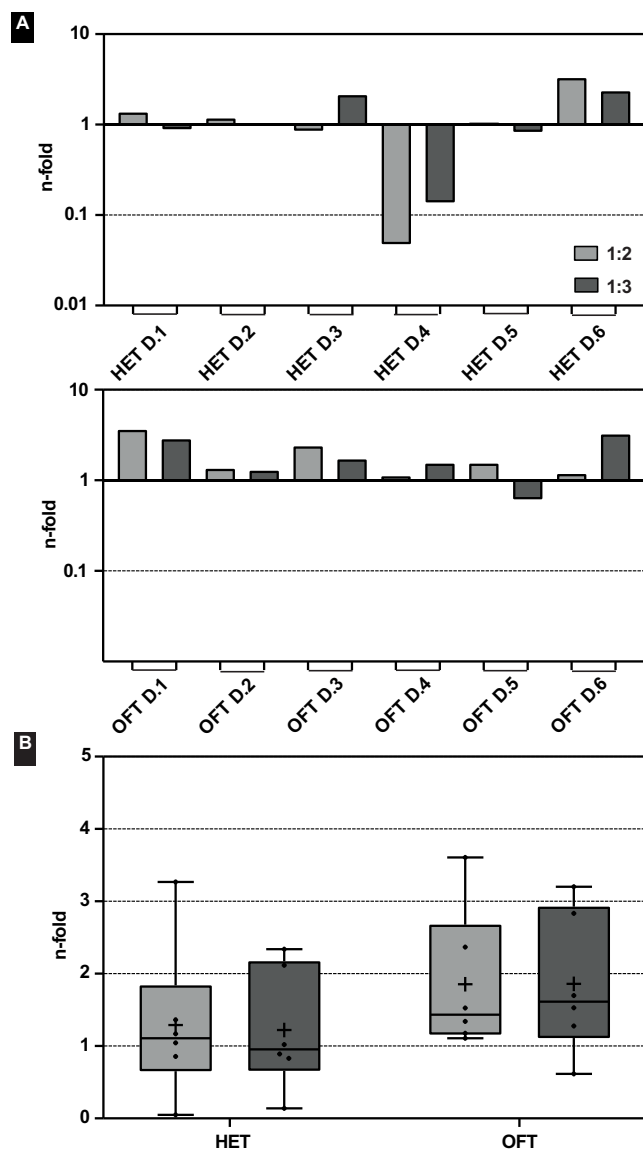


Figure 13: A: Measurement of increase or decrease in osteogenic differentiation potential, comparing monocultures at a ratio of 1:0 to co-cultures at ratios of 1:2 and 1:3. The HET group (A) showed a positive influence of osteogenic differentiation in the co-cultures for several donor samples (e.g: HET D.3 and D.6). However, some donor samples (e.g: HET D.4 and D.5) showed a lowered or unaltered potential. The OFT group was positively influenced in co-cultures for all donor samples, except one (OFT D.5 at ratio 1:3) B: When HET and OFT donors were paired into groups, a non-significant change was seen for the HET group ($p=0.904$) when comparing osteogenic differentiation potential in co-cultures at 1:2 and 1:3 ratio. The same result was seen for the OFT group ($p=0.993$), whereby there was a non-significant difference when comparing 1:2 and 1:3 ratio. Comparing the HET group to the OFT group a significant change was not observed in either 1:2 or the 1:3 groups ($p=0.362$ at ratio 1:2, $p=0.254$ at ratio 1:3). Graph:Box and whisker plot (min and max point) with median (line) and mean (+). Only significant changes are represented graphically.

3.4 hUVEC survival and morphology changes under co-cultures

During the period of osteogenic differentiation, the morphology and formation of hUVECs were examined using their overexpression of green fluorescent protein characteristic. Figure 14 shows the cell shape of UVECs in co-cultures with two different donors and the corresponding control groups. These cell shapes were observed on days 3, 7, 10 and 14 of osteogenic differentiation. Cell survival varied with an average of 7.3 ± 5.3 days for both groups.

Figure 14 demonstrates exemplary images of hUVECs morphology and formation on day 14 of osteogenic differentiation. The figures show different co-culture ratios during osteogenic differentiation (A and B) and control groups (C and D). hUVECs during osteogenic differentiation (A and B) showed an increased accumulation and the cell structure seemed rounder, whereas hUVECs in the control group expanded more and the cell structure appeared more flattened.

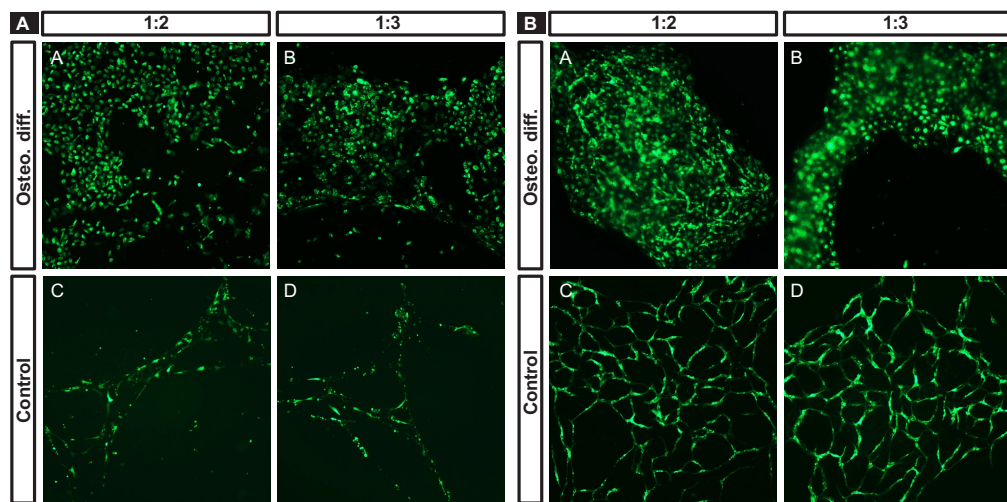


Figure 14: Exemplary microscopy images on day 14 of osteogenic differentiation, presenting hUVECs morphology in co-culture (1:2, 1:3) A. HET D.4 B.OFT D.2. During osteogenic differentiation cell formation (A and B) showed an increased accumulation and the cell structure seemed rounder, whereas hUVECs in the control group expanded more and the cell structure appeared more flattened. Bar equals 100 μ m

4 Discussion

Bone-tissue-engineering has evolved tremendously in recent years. However, vascularization, low oxygen levels and sufficient osteogenic differentiation potential remain problems. Until now, cell culture experiments have been performed at an oxygen concentration of 20% , although this does not correspond with the physiological concentration in most tissues. There have been no exact results concerning oxygen concentration in the bone itself, but oxygen concentrations in the bone cell niche have been estimated between 1 and 6% [42] and can range from 5 to 12.5% in bone tissue [43].

As vascularization is the key to oxygenation, the interaction between MSCs and angiogenesis requires further evaluation. Moreover, bone regulation in unhealthy bone tissue (e.g. osteoporosis) remains rather uncharted and is therefore an important subject of future research. In the present study, growth characteristics, morphological differences and osteogenic differentiation from primary human mesenchymal stem cells, obtained from patients with a high-energy trauma or a osteoporotic-fracture trauma, were evaluated. To evaluate the importance of oxygen concentrations, cells were seeded in 21% (normoxic) and 2% (hypoxic) oxygen concentrations. To evaluate the interaction between angiogenesis and osteogenic differentiation, hMSCs were co-cultured with hUVECs at different ratios.

4.1 Biological cell characteristics

4.1.1 Cell morphology

Cell morphology has been commonly described by the cell's structure, shape, size and some other features. Over the last decade, the morphology of hMSCs in particular has been analyzed in different circumstances and over different time periods. Morphologically, hMSCs could be separated into three major groups: rapidly self-renewing cells; elongated, fibroblastic-like, spindle-shaped cells and slowly replicating; large, cuboidal or flattened cells [95]. Certain cell shapes have been associated with different characteristics. Colter et al. demonstrated that flattened cells represent more mature hMSCs. This kind of cell type has often been described in the context of senescence, additionally appearing vacuolized and with enlarged nuclei [96, 97]. In 1960, Hayflick and Moorhead first described senescence as "an essentially irreversible arrest of cell division". Cells remain alive, despite the loss of function [97]. The correlation between alkaline phosphatase activity and morphology has suggested, that flattened cells represent the early stages of osteogenic progenitor cells [98]. Rapidly self-renewing cells, on the other hand, appear to have multilineage proprieties and present early progenitors [95, 99, 100].

In the context of this work, it was important to gain a better understanding of the impact of oxygen concentrations on cell morphology, to progress the research on tissue engineering and the related disease treatments. As mentioned previously, hMSCs were seeded in two different oxygen concentrations, normoxic (21% O₂) and hypoxic (2% O₂), and their cell morphology was evaluated. During the first couple of days, cell morphology was almost indistinguishable between the two oxygen levels. Nonetheless, cells in 2% O₂ showed flattening at a later stage than cells in 21% O₂. Especially for the HET group, area measurements in hypoxia were significantly smaller than in normoxia on days 10 and 20. For the OFT group, this tendency was evident, although it was non-significant. Several studies have shown a similar behaviour in hMSCs. Fehrer et al., demonstrated that in lower passages,

cell morphology was equal for 20% oxygen and 3% oxygen. Cells cultured in 3% kept their spindle-shape longer than cells cultured in normoxia, which led to flattened and enlarged cells at an earlier stage [101]. The same results were shown by Grayson et al., in hypoxia cells kept a spindle-shape and had a higher density. Contrary to this, in normoxia, cell shape has been shown to change into a flattened and broader shape earlier, either indicating senescence or cell differentiation [102]. To further investigate if hypoxia has an influence on senescence, Kwon et al. used a β -galactosidase staining kit to evaluate senescence in hypoxia and normoxia, showing that hypoxia prevented senescence [103]. Due to time constraints, such a procedure was not performed in this work.

Moreover, as mentioned in the hypothesis section of this thesis, age-related differences were analyzed. Interestingly, area measurements in the HET group in normoxia on day 10 tended to be bigger as in the HET hypoxia or OFT group (normoxia and hypoxia). Contrary to this result, Baxter et al. showed, the number of flattened and slowly proliferating cells increases with rising donor age [104]. Moreover, the different oxygen levels had a stronger impact on the HET group than on the OFT group, showing significant differences in hypoxia to normoxia. The influence of oxygen concentration on hMSCs of different age groups has not been researched a lot and therefore investigation has to be done.

4.1.2 Proliferation of hMSCs in different oxygen levels

As for the previous chapter, cultural conditions need to be evaluated in order to improve BTE applications. In vitro expansion of hMSCs needs to be optimized, to achieve a high cell number for transplants. A high cell number can be achieved with optimal cell culture conditions. Therefore, cumulative population doublings were examined. In the beginning, the results for all twelve donor samples showed a similar curve in normoxic and hypoxic conditions. In the following days, the results showed decreased cumulative population doubling and a ceasing of proliferation, mostly after 20 days. Donor hMSCs showed a higher, but non-significant, proliferation rate in hypoxic conditions, compared to normoxic conditions. The exact repercussions of oxygen concentrations on hMSCs have not been fully understood, although several studies have demonstrated the positive effects on cell proliferation [44, 105, 106]. Fehrer and colleagues even showed that cells cultured in 21% O_2 concentrations ceased growing earlier and entered senescence, whereas cells cultured in lower O_2 concentrations (3%), continued proliferation. Fehrer's PD values were much higher than the cumPD figures calculated in the present thesis. The PD discrepancy might be due to the negative impact of cryopreservation on proliferation, as proven in several studies [107]. Additionally, higher passages might be a reason. Moreover, reduced oxygen, which is closer to their natural habitat, attenuates the differentiation capacity of human mesenchymal stem cells, prolongs their lifespan [101] and reduces chromosomal abnormalities and DNA damages [108]. Different pathways, such as triggering a higher proliferation capacity in hypoxic conditions, upregulating Notch target genes, activating the HIF-alpha pathway and decreasing reactive oxygen species [105, 109], have been discovered. The HIF-pathway plays an important role in osteogenesis, angiogenesis and gene regulation. Buizer et al. attempted to identify the optimal oxygen concentration at which cell proliferation and angiogenetic factors were both increased. HIF1-a has been shown to enhance the synthesis of angiogenetic factors (e.g VEGF, FGF). Buizer et al have observed that oxygen levels of approximately 1-2% induced the highest proliferation

and expression of VEGF [110]. However, Holzwath and colleagues demonstrated a negative impact on cell proliferation in 1% oxygen [111]. Differences in the experimental setup, for example, duration of hypoxia, level of O₂ and preconditioning make it difficult to compare this studies.

Our study further investigated the impact of age and osteoporosis on proliferation capacity by comparing HET to OFT hMSCs. Grouping the donor samples into two age categories (HET and OFT), our results demonstrated no significant changes concerning proliferation. Some of the young donor samples (HET D.6, age 20) showed a lower proliferation capacity than older donors (e.g. OFT D.6, age 93) These results match the findings of Justesen and his colleagues [112], who stated that no correlation could be made between decreased proliferation and age. Additionally, Justesen and colleagues showed that osteoporotic hMSCs did not differ from age-matched non-osteoporotic donors, concerning proliferation. Nonetheless, a decreased proliferation capacity has been previously mentioned in literature [113–115]. These discrepancies in literature show how important it is to find the ideal culture conditions for hMSCs and to gain a better understanding of the effect of aging and osteoporosis on proliferation.

4.2 Osteogenic differentiation potential in different oxygen concentrations

Within fracture healing, hypoxia has been shown to play an important role in osteogenesis and angiogenesis. In the early stages of fracture healing, hypoxia activates the HIF-1a pathway, thereby stimulating angiogenesis and osteogenesis [55]. However, the exact molecular mechanisms and the interaction between all cells involved in fracture healing, remain insufficiently explored, despite being a key element of BTE. In our study, all donors showed a better osteogenic differentiation potential in normoxic cell culture conditions than in hypoxia. This result corresponds to numerous other studies [116–118]. A body of evidence has shown, that continuous hypoxic conditions decrease the osteogenic differentiation potential due to Notch signal activation [116, 119] and decrease the Runx2 signal. Runx2 being a marker for osteogenic differentiation. In our experiment cells were seeded in normoxia until a high density was reached, before being put into hypoxia and normoxia for the whole process of osteogenic differentiation (21 days). Similar results were obtained regarding enhancing osteogenic differentiation in normoxia. On the contrary, Genetos et al. discovered, that 48 hours of hypoxia enhances osteogenesis by activating the Wnt signal [120]. Yu et al. recorded the same result after three days of hypoxia [121]. This discrepancy shows that the role of the HIF-1a-interplay in osteogenic differentiation is still not fully understood and timing of cell culture condition in hypoxia and normoxia for gaining the best results requires further examination.

As outlined in the previous two chapters, age has also been of interest in the context of osteogenic differentiation. Referring to the questions from the hypothesis, if there were differences in the HET and the OFT groups concerning osteogenic differentiation potential, no significant change was seen. However, a tendency was detected for the HET group towards a stronger differentiation potential. In the literature, the influence of aging on osteogenic differentiation capacity has generated different results. Zaim and colleagues [122] showed a correlation between decreased osteogenic differentiation capacity and age, as did other studies [123,124]. In contrast, other research teams presented no correlation between osteogenic differentiation potential and age [125, 126]. Contrary to the aforementioned studies, the

OFT hMSCs in our experiment were not only from aged, but additionally from osteoporotic donors. Studies have suggested that the osteogenic differentiation potential of osteoporotic bone is attenuated [127, 128]. Miyamoto et al. reported that HIF-1a could be an essential factor in osteoporosis by accumulating and activating osteoclasts. [129, 130] Recent studies have found that post-menopausal osteoblast cell lines are differently affected by oxidative stress and hypoxia than healthy osteoblasts. Epigenetic changes, such as downregulation of histone acetyltransferase 1, KAT5, histone deacetylase 6, have been found to occur, especially in chromatin-modifying enzymes. Histone acetyltransferase 1 is important for osteogenesis and histone deacetylase 6 correlates with angiogenesis [131]. Publications have shown, that hypoxia can increase or decrease the osteogenic differentiation potential, depending on the duration and level of O₂ [116–118, 122], further investigations to find the optimal oxygen concentration for osteogenic differentiation are needed. Moreover, it has been shown that hypoxia can have a different influence on the osteogenic differentiation potential on young, aged and osteoporotic hMSCs.

4.3 Osteogenic differentiation potential in co-culture

As osteogenesis and angiogenesis are both pillars of bone regeneration, in this study, a co-culture with hMSCs and hUVECs was established. The osteogenic differentiation potential in different co-culture conditions was observed, and more precisely, the co-culture's impact on OFT hMSCs was compared with HET hMSCs. Both groups showed improved osteogenic differentiation potential in co-cultures as compared with monocultures. However, the differences in the ratios (hMSCs:hUVECs) of 1:2 and 1:3 proved to be insignificant. Previous studies have elucidated the positive effects of co-cultures of MSCs and UVECs on osteogenesis and cell proliferation [86, 91, 132–134]. A mutual relationship through cell-cell-communication (direct communication, gap-junctions and paracrine effects) has been reported in the literature. Direct communication has been shown to be influenced by co-cultures, which enhance the expressions of members of the cadherin family (VE-cadherin and N-Cadherin), increase ALP expression, increase type I collagen and promote vessel formation [108, 132]. Diffusible factors produced by endothelial cells, such as BMP-2, insulin-like-growth factor and endothelin-1 are upregulated by the co-culture and influence osteogenesis and proliferation [91, 135]. In turn, as Chen et al. showed, hMSCs and osteoblasts secrete VEGF and other growth factors [132]. Additionally, extracellular matrix has been identified as having a key role in communication through its capacity to store and secrete growth factors, chemokines and enzymes produced by hMSCs and endothelial cells. Another approach concerning co-cultures, is to identify the right balance between the mediums used. Many research groups such as Villar et al. [136] used one medium, either for osteogenic or angiogenic differentiation. In 2011 Ma et al. [137] presented their project on a co-culture with a mixed medium, showing that only osteogenic medium can induce mineralization, while mixed or endothelial medium cannot. However in this experiment, it was shown that both cell types (hMSCs and hUVECs) were able to survive and induce osteogenic differentiation by preculturing in ECGM until the necessary density was attained, followed by culturing in the inducing medium.

As mentioned in the hypothesis section of this thesis, age-related differences were analyzed. For the first time it was shown that aged donors, in this context the OFT group, showed a tendency towards greater influence from the co-cultures compared to the HET group. Since the donors used in

this experiment were aged and had osteoporosis, it would be interesting to investigate if this effect is mostly due to the age or the osteoporosis. And further to investigate the interactions being responsible for this effect.

Finally, to take further step towards BTE, a 3D co-culture was tested. So far, many 3D models have been tested and different problems detected. [138–140]. Moreover, *in vivo* studies present the next step in BTE, although they remain limited in number thus far. Zhang and colleagues [141] showed that mineralization and vascularization were induced in a collagen hydrogel scaffold seeded with MSCs and hUVECs. However, no ectopic bone formation was seen. To the contrary, *in vivo* studies by Liu et al. [138] showed, that co-seeded scaffolds were able to induce the formation of new bone in rats. In the study performed for this thesis, an approach towards a 3D model was examined, however the results were not conclusive enough (figure 17 and 18). A drastic shrinkage of the scaffold was observed over the cultivating time, slightly more pronounced under osteogenic differentiation, suggesting cell interaction or growth. In order to be sure of cell survival, a cell survival test was performed at the end and showed that cells were able to survive 14 days on the scaffold. The previous results are a step in the right direction and show that mineralization and vascularization in co-cultures are possible. Many studies have been conducted regarding co-cultures; however, drastically different approaches have rendered it difficult to find a consensus on the optimal conditions. Therefore, co-culture conditions, such as ratio, medium, oxygen levels, pre-conditioning, usage of growth factors or influence of *in vivo* culturing, still need to be optimized.

4.4 Morphological changes of hUVECs and their role in bone tissue engineering

Vascular network are important for oxygen transportation and nutrition. Our research demonstrated that hUVECs were, despite decreasing numbers, able to survive until day 14 in several co-cultures and had a positive effect on osteogenesis. On the other hand, hUVECs cultured in monocultures only survived until day 3 in the medium for osteogenic differentiation, suggesting that somehow hMSCs and hUVECs have a positive influence on one another's survival. To further improve osteogenic differentiation, BMP2 was added to the osteogenic differentiation medium for the co-culture experiment, due to positive effects already demonstrated by Prall et al. [128]. Analyzing the morphology of the hUVECs, the shape and formation were different in the osteogenic differentiation medium than in the control group. hUVECs seemed rounder in shape and had higher accumulation when seeded in co-culture and being induced to osteogenic differentiation, it almost seemed as they would form a 3D-like structure, which Fuchs et al referred to as a lumen-like structure [142]. hUVECs were first used to reconstruct a capillary-like network by Black et al. in 1998, which shows that the idea of hUVECs restoring or inducing vascularization is not new [143]. Regarding to the importance of VEGF, Zhang et al. [144] showed that VEGF is also upregulated in co-cultures, seeded in hypoxic cell culture conditions. Consequently, the angiogenic ability of hUVECs was higher. Many *in vitro* and *in vivo* studies on vascularization induced by hUVECs in co-cultures, have been undertaken. *In vivo* studies done by Koike et al. [145] presented the successful formation of blood vessels by implanting a fibronectin-type-I collagen gel scaffold, seeded with hUVECs and mesenchymal precursor cells. The formed network connected to the mouse's vascular system. One year after transplantation, the functionality and stability of the network were still intact. Re-

cently, 3D bioprinting has shown promising results in prevascularized scaffolds, with capability for inducing angio- and osteogenesis [146, 147]. Data on optimal conditions, medium, oxygen concentrations and ratios are still lacking, and more specific knowledge needs to be acquired in this context.

4.5 Critical discussion of the experimental setup

When conducting a research study, it is important to consider the size of the sample used. In this study, twelve individual donors were used for all the experiments. The negative effects of a small sample size are a lack of diversity and representation of the population of interest and difficulty detecting significant effects or differences between groups caused due to the low statistical power. This low statistical power was in evidence throughout the study, as almost all results were non-significant and donor dependency manifested. In most cases, a tendency was seen, for example a higher proliferation in hypoxia, a better osteogenic differentiation in normoxia or a higher ARS deposition for the HET group than OFT group. It can be assumed that the results would have been more significant with a higher donor number of donor samples. Donor availability, especially for younger donors was limited and it took many months to gather the samples. Additionally, a higher donor number would also have surpassed the timeframe scheduled for this work. Another critical point to discuss is the two different groups, HET and OFT. The donors were only randomized by their age and the diagnose of osteoporosis. However for the younger donors (HET group), no osteodensitometry and therefore no T-score values were available. Looking at the results in relation to the age, a tendency towards better proliferation and higher osteogenic differentiation was seen for the HET group. However, considering the individual donor samples, some aged donors performed better than young donors, for example, when looking at the CFU results OFT D.1, suggesting that there might be factors aside from age to consider when randomizing donor samples into groups. Further, there were no aged and healthy donor samples to compare the results to.

Another limitation to the study was the experimental setup, as a high number of cells were required and donors responded to cell growth uniquely. Some donors had a higher passage in the different experiments.

5 Conclusion and Outlook

The results of the experiments performed for this study indicate that oxygen concentrations have an impact on cell morphology, proliferation and osteogenic differentiation potential. Hypoxia induces a tendency towards increased proliferation and decreased osteogenic differentiation potential. Additionally, it was demonstrated that co-cultures have an impact on mineralization, trending towards enhancement. Furthermore, the results show that HET and OFT hMSCs in co-cultures have a different impact on their osteogenic differentiation potential, whereas the OFT group expressed a trend towards a stronger influence. In a future study, it would be interesting to discover the right amount of oxygen level to improve the balance of proliferation, multilineage, lifespan and osteogenic differentiation potential. Moreover, the investigation of the effect of different medium compositions on the osteogenic differentiation potential and vessel formation in co-cultures needs to be looked at. Finally, it would be interesting to explore the impact of hypoxia on the proliferation of co-culture's and UVEC's, as well as vessel formation. The aim would be to gain further information on cell-cell interac-

tion and improve culture conditions. In the opinion of the researcher, more knowledge about the complexity of oxygen levels and co-cultures is required to sustain cell viability, osteogenesis and angiogenesis in order to improve BTE and thereby take a step forward towards the treatment of critical size bone-defects.

6 References

References

- [1] Consensus Development Conference, "Consensus development conference: Diagnosis, prophylaxis, and treatment of osteoporosis," *The American Journal of Medicine*, vol. 94, pp. 646–650, jun 1993.
- [2] M. B. Greenblatt, J. N. Tsai, and M. N. Wein, "Bone Turnover Markers in the Diagnosis and Monitoring of Metabolic Bone Disease," *Clinical Chemistry*, vol. 63, pp. 464–474, feb 2017.
- [3] P. Hadji, S. Klein, H. Gothe, B. Häussler, T. Kless, T. Schmidt, T. Steinle, F. Verheyen, and R. Linder, "The epidemiology of osteoporosis—Bone Evaluation Study (BEST): an analysis of routine health insurance data.," *Deutsches Aerzteblatt Online*, jan 2013.
- [4] T. Urano and S. Inoue, "Genetics of osteoporosis," *Biochemical and Biophysical Research Communications*, vol. 452, pp. 287–293, sep 2014.
- [5] A. Aibar-Almazán, A. Voltes-Martínez, Y. Castellote-Caballero, D. F. Afanador-Restrepo, M. d. C. Carcelén-Fraile, and E. López-Ruiz, "Current Status of the Diagnosis and Management of Osteoporosis," *International Journal of Molecular Sciences*, vol. 23, no. 16, pp. 1–27, 2022.
- [6] D. L. Glaser and F. S. Kaplan, "Osteoporosis," *Spine*, vol. 22, pp. 12S–16S, dec 1997.
- [7] J. Kanis, C. Cooper, R. Rizzoli, and J.-Y. Reginster, "European guidance for the diagnosis and management of osteoporosis in post-menopausal women," *Osteoporosis International*, vol. 30, pp. 3–44, jan 2019.
- [8] K. Engelke and C. C. Glüer, "Quality and performance measures in bone densitometry: part 1: errors and diagnosis.," *Osteoporosis international : a journal established as result of cooperation between the European Foundation for Osteoporosis and the National Osteoporosis Foundation of the USA*, vol. 17, no. 9, pp. 1283–1292, 2006.
- [9] C. C. Glüer, Y. Lu, and K. Engelke, "Quality and performance measures in bone densitometry - Part 2: Fracture risk," *Osteoporosis International*, vol. 17, no. 10, pp. 1449–1458, 2006.
- [10] G. M. Blake and I. Fogelman, "The role of DXA bone density scans in the diagnosis and treatment of osteoporosis," *Postgraduate Medical Journal*, vol. 83, no. 982, pp. 509–517, 2007.
- [11] J. A. Kanis, "Diagnosis of osteoporosis and assessment of fracture risk," *The Lancet*, vol. 359, pp. 1929–1936, 2002.
- [12] P. D. Delmas, R. Eastell, P. Garnero, M. J. Seibel, and J. Stepan, "The Use of Biochemical Markers of Bone Turnover in Osteoporosis," *Osteoporosis International*, vol. 11, pp. S2–S17, dec 2000.
- [13] E. Stein and E. Shane, "Secondary osteoporosis," *Endocrinology and Metabolism Clinics of North America*, vol. 32, no. 1, pp. 115–134, 2003.

- [14] S. Ferrari, M. L. Bianchi, J. A. Eisman, A. J. Foldes, S. Adami, D. A. Wahl, J. J. Stepan, M. C. De Vernejoul, and J. M. Kaufman, "Osteoporosis in young adults: Pathophysiology, diagnosis, and management," *Osteoporosis International*, vol. 23, no. 12, pp. 2735–2748, 2012.
- [15] J. A. Kanis, N. C. Harvey, H. Johansson, E. Liu, L. Vandenput, M. Lorentzon, W. D. Leslie, and E. V. McCloskey, "A decade of FRAX: how has it changed the management of osteoporosis?," *Aging Clinical and Experimental Research*, vol. 32, pp. 187–196, feb 2020.
- [16] S. H. Tella and J. C. Gallagher, "Prevention and treatment of postmenopausal osteoporosis," *Journal of Steroid Biochemistry and Molecular Biology*, vol. 142, pp. 155–170, 2014.
- [17] R. P. Heaney, T. M. Zizic, I. Fogelman, W. P. Olszynski, P. Geusens, C. Kasibhatla, N. Alsayed, G. Isaia, M. W. Davie, and C. H. Chesnut, "Risedronate reduces the risk of first vertebral fracture in osteoporotic women," *Osteoporosis International*, vol. 13, no. 6, pp. 501–505, 2002.
- [18] P. D. Delmas, "Treatment of postmenopausal osteoporosis," *The Lancet*, vol. 359, no. 9322, pp. 2018–2026, 2002.
- [19] J. Liu, E. M. Curtis, C. Cooper, and N. C. Harvey, "State of the art in osteoporosis risk assessment and treatment," *Journal of Endocrinological Investigation*, vol. 42, pp. 1149–1164, oct 2019.
- [20] B. Arjmand, M. Sarvari, S. Alavi-Moghadam, M. Payab, P. Goodarzi, K. Gilany, N. Mehrdad, and B. Larijani, "Prospect of Stem Cell Therapy and Regenerative Medicine in Osteoporosis," *Frontiers in Endocrinology*, vol. 11, no. July, pp. 1–9, 2020.
- [21] N. Imamudeen, A. Basheer, A. M. Iqbal, N. Manjila, N. N. Haroon, and S. Manjila, "Management of Osteoporosis and Spinal Fractures: Contemporary Guidelines and Evolving Paradigms," *Clinical Medicine and Research*, vol. 20, no. 2, pp. 95–106, 2022.
- [22] H. Xie, Z. Cui, L. Wang, Z. Xia, Y. Hu, L. Xian, C. Li, L. Xie, J. Crane, M. Wan, G. Zhen, Q. Bian, B. Yu, W. Chang, T. Qiu, M. Pickarski, L. T. Duong, J. J. Windle, X. Luo, E. Liao, and X. Cao, "PDGF-BB secreted by preosteoclasts induces angiogenesis during coupling with osteogenesis," *Nature Medicine*, vol. 20, pp. 1270–1278, nov 2014.
- [23] M. T. Valenti, L. Dalle Carbonare, and M. Mottes, "Osteogenic Differentiation in Healthy and Pathological Conditions," *International journal of molecular sciences*, vol. 18, no. 1, 2016.
- [24] M. T. Valenti, U. Garbin, A. Pasini, M. Zanatta, C. Stranieri, S. Manfro, C. Zucal, and L. Dalle Carbonare, "Role of Ox-PAPCs in the Differentiation of Mesenchymal Stem Cells (MSCs) and Runx2 and PPAR γ 2 Expression in MSCs-Like of Osteoporotic Patients," *PLoS ONE*, vol. 6, p. e20363, jun 2011.
- [25] S. C. Manolagas, "From Estrogen-Centric to Aging and Oxidative Stress: A Revised Perspective of the Pathogenesis of Osteoporosis," *Endocrine Reviews*, vol. 31, pp. 266–300, jun 2010.

- [26] A. M. Pino, C. J. Rosen, and J. P. Rodríguez, “In Osteoporosis, differentiation of mesenchymal stem cells (MSCs) improves bone marrow adipogenesis,” *Biological Research*, vol. 45, no. 3, pp. 279–287, 2012.
- [27] S. Stegen and G. Carmeliet, “The skeletal vascular system – Breathing life into bone tissue,” *Bone*, vol. 115, pp. 50–58, 2018.
- [28] S. K. Ramasamy, A. P. Kusumbe, M. Schiller, D. Zeuschner, M. G. Bixel, C. Milia, J. Gamrekelashvili, A. Limbourg, A. Medvinsky, M. M. Santoro, F. P. Limbourg, and R. H. Adams, “Blood flow controls bone vascular function and osteogenesis,” *Nature Communications*, vol. 7, pp. 1–13, 2016.
- [29] J. Y. Rho, L. Kuhn-Spearing, and P. Ziopoulos, “Mechanical properties and the hierarchical structure of bone,” *Medical Engineering and Physics*, vol. 20, no. 2, pp. 92–102, 1998.
- [30] M. Bartold, S. Gronthos, D. Haynes, and S. Ivanovski, “Mesenchymal stem cells and biologic factors leading to bone formation,” *Journal of Clinical Periodontology*, vol. 46, no. S21, pp. 12–32, 2019.
- [31] B. K. Hall and T. Miyake, “Divide, accumulate, differentiate: cell condensation in skeletal development revisited.,” *The International journal of developmental biology*, vol. 39, pp. 881–93, dec 1995.
- [32] A. D. Berendsen and B. R. Olsen, “Bone development,” *Bone*, vol. 80, pp. 14–18, nov 2015.
- [33] A. Erlebacher, E. H. Filvaroff, S. E. Gitelman, and R. Derynck, “Toward a molecular understanding of skeletal development,” *Cell*, vol. 80, pp. 371–378, feb 1995.
- [34] C. M. Runyan and K. S. Gabrick, “Biology of bone formation, fracture healing, and distraction osteogenesis,” *Journal of Craniofacial Surgery*, vol. 28, no. 5, pp. 1380–1389, 2017.
- [35] E. J. Mackie, Y. A. Ahmed, L. Tatarczuch, K. S. Chen, and M. Mirams, “Endochondral ossification: How cartilage is converted into bone in the developing skeleton,” *International Journal of Biochemistry and Cell Biology*, vol. 40, no. 1, pp. 46–62, 2008.
- [36] S. M. Walzer, E. Cetin, R. Grübl-Barabas, I. Sulzbacher, B. Rueger, W. Girsch, S. Toegel, R. Windhager, and M. B. Fischer, “Vascularization of primary and secondary ossification centres in the human growth plate,” *BMC Developmental Biology*, vol. 14, no. 1, pp. 1–12, 2014.
- [37] C. Maes, T. Kobayashi, M. K. Selig, S. Torrekens, S. I. Roth, S. Mackem, G. Carmeliet, and H. M. Kronenberg, “Osteoblast Precursors, but Not Mature Osteoblasts, Move into Developing and Fractured Bones along with Invading Blood Vessels,” *Developmental Cell*, vol. 19, pp. 329–344, aug 2010.
- [38] G. Karsenty, “The complexities of skeletal biology,” *Nature*, vol. 423, pp. 316–318, may 2003.
- [39] M. L. Brandi and P. Collin-Osdoby, “Vascular Biology and the Skeleton,” *Journal of Bone and Mineral Research*, vol. 21, pp. 183–192, feb 2006.

[40] P. Katsimbri, "The biology of normal bone remodelling," *European Journal of Cancer Care*, vol. 26, p. e12740, nov 2017.

[41] R. E. Tomlinson and M. J. Silva, "Skeletal Blood Flow in Bone Repair and Maintenance," *Bone Research*, vol. 1, pp. 311–322, dec 2013.

[42] J.-S. Lee, J.-C. Park, T.-W. Kim, B.-J. Jung, Y. Lee, E.-K. Shim, S. Park, E.-Y. Choi, K.-S. Cho, and C.-S. Kim, "Human bone marrow stem cells cultured under hypoxic conditions present altered characteristics and enhanced *in vivo* tissue regeneration," *Bone*, vol. 78, pp. 34–45, 2015.

[43] E. J. Sheehy, C. T. Buckley, and D. J. Kelly, "Oxygen tension regulates the osteogenic, chondrogenic and endochondral phenotype of bone marrow derived mesenchymal stem cells," *Biochemical and Biophysical Research Communications*, vol. 417, pp. 305–310, jan 2012.

[44] E. Potier, E. Ferreira, R. Andriamanalijaona, J.-P. Pujol, K. Oudina, D. Logeart-Avramoglou, and H. Petite, "Hypoxia affects mesenchymal stromal cell osteogenic differentiation and angiogenic factor expression," *Bone*, vol. 40, pp. 1078–1087, apr 2007.

[45] J. Filipowska, K. A. Tomaszewski, Ł. Niedźwiedzki, J. A. Walocha, and T. Niedźwiedzki, "The role of vasculature in bone development, regeneration and proper systemic functioning," *Angiogenesis*, vol. 20, pp. 291–302, aug 2017.

[46] C. J. Percival and J. T. Richtsmeier, "Angiogenesis and intramembranous osteogenesis," *Developmental Dynamics*, vol. 242, pp. 909–922, aug 2013.

[47] W. Risau and I. Flamme, "Vasculogenesis," *Annual Review of Cell and Developmental Biology*, vol. 11, pp. 73–91, nov 1995.

[48] K. K. Sivaraj and R. H. Adams, "Blood vessel formation and function in bone," *Development*, vol. 143, pp. 2706–2715, aug 2016.

[49] K. Hu and B. R. Olsen, "Osteoblast-derived VEGF regulates osteoblast differentiation and bone formation during bone repair," *Journal of Clinical Investigation*, vol. 126, pp. 509–526, jan 2016.

[50] K. Hu and B. R. Olsen, "The roles of vascular endothelial growth factor in bone repair and regeneration," *Bone*, vol. 91, pp. 30–38, 2016.

[51] E. Araldi and E. Schipani, "Hypoxia, HIFs and bone development," *Bone*, vol. 47, pp. 190–196, aug 2010.

[52] B. L. Krock, N. Skuli, and M. C. Simon, "Hypoxia-Induced Angiogenesis: Good and Evil," *Genes and Cancer*, vol. 2, no. 12, pp. 1117–1133, 2011.

[53] C. Wan, J. Shao, S. R. Gilbert, R. C. Riddle, F. Long, R. S. Johnson, E. Schipani, and T. L. Clemens, "Role of HIF-1 α in skeletal development," *Annals of the New York Academy of Sciences*, vol. 1192, pp. 322–326, apr 2010.

[54] J. C. Utting, S. P. Robins, A. Branda-Burch, I. R. Orriss, J. Behar, and T. R. Arnett, "Hypoxia inhibits the growth, differentiation and bone-forming capacity of rat osteoblasts," *Experimental Cell Research*, vol. 312, no. 10, pp. 1693–1702, 2006.

[55] Y. Wang, C. Wan, L. Deng, X. Liu, X. Cao, S. R. Gilbert, M. L. Bouxsein, M. C. Faugere, R. E. Guldberg, L. C. Gerstenfeld, V. H. Haase, R. S. Johnson, E. Schipani, and T. L. Clemens, “The hypoxia-inducible factor α pathway couples angiogenesis to osteogenesis during skeletal development,” *Journal of Clinical Investigation*, vol. 117, no. 6, pp. 1616–1626, 2007.

[56] Z. Ungvari, S. Tarantini, F. Sorond, B. Merkely, and A. Csiszar, “Mechanisms of Vascular Aging, A Geroscience Perspective: JACC Focus Seminar,” *Journal of the American College of Cardiology*, vol. 75, no. 8, pp. 931–941, 2020.

[57] M. T. Vogt, J. A. Cauley, L. H. Kuller, and M. C. Nevitt, “Bone Mineral Density and Blood Flow to the Lower Extremities: The Study of Osteoporotic Fractures,” *Journal of Bone and Mineral Research*, vol. 12, pp. 283–289, feb 1997.

[58] R. Florencio-Silva, G. R. D. S. Sasso, E. Sasso-Cerri, M. J. Simões, and P. S. Cerri, “Biology of Bone Tissue: Structure, Function, and Factors That Influence Bone Cells,” *BioMed Research International*, vol. 2015, pp. 1–17, 2015.

[59] J. Belinha, *Meshless Methods in Biomechanics: Bone Tissue Remodelling Analysis. Lecture Notes in Computational Vision and Biomechanics*. 2014.

[60] X. Feng, “Chemical and Biochemical Basis of Cell-Bone Matrix Interaction in Health and Disease,” *Current Chemical Biology*, vol. 3, pp. 189–196, may 2009.

[61] M. Unal, A. Creecy, and J. S. Nyman, “The Role of Matrix Composition in the Mechanical Behavior of Bone,” *Current Osteoporosis Reports*, vol. 16, pp. 205–215, jun 2018.

[62] H. Fonseca, D. Moreira-Gonçalves, H.-J. A. Coriolano, and J. A. Duarte, “Bone Quality: The Determinants of Bone Strength and Fragility,” *Sports Medicine*, vol. 44, pp. 37–53, jan 2014.

[63] B. Liang, G. Burley, S. Lin, and Y. C. Shi, “Osteoporosis pathogenesis and treatment: existing and emerging avenues,” *Cellular and Molecular Biology Letters*, vol. 27, no. 1, 2022.

[64] W. J. Boyle, W. S. Simonet, and D. L. Lacey, “Osteoclast differentiation and activation,” *Nature*, vol. 423, pp. 337–342, may 2003.

[65] S. L. Dallas, M. Prideaux, and L. F. Bonewald, “The Osteocyte: An Endocrine Cell ... and More,” *Endocrine Reviews*, vol. 34, pp. 658–690, oct 2013.

[66] V. Everts, J. M. Delaissé, W. Korper, D. C. Jansen, W. Tigchelaar-Gutter, P. Saftig, and W. Beertsen, “The Bone Lining Cell: Its Role in Cleaning Howship’s Lacunae and Initiating Bone Formation,” *Journal of Bone and Mineral Research*, vol. 17, pp. 77–90, jan 2002.

[67] T. L. Andersen, T. E. Sondergaard, K. E. Skorzynska, F. Dagnaes-Hansen, T. L. Plesner, E. M. Hauge, T. Plesner, and J.-M. Delaisse, “A Physical Mechanism for Coupling Bone Resorption and Formation in Adult Human Bone,” *The American Journal of Pathology*, vol. 174, pp. 239–247, jan 2009.

- [68] I. H. Kalfas, "Principles of bone healing," *Neurosurgical Focus*, vol. 10, pp. 1–4, apr 2001.
- [69] S. Huang, M. Jin, N. Su, and L. Chen, "New insights on the reparative cells in bone regeneration and repair," *Biological Reviews*, vol. 96, no. 2, pp. 357–375, 2021.
- [70] J. Goldhahn, J. M. Féron, J. Kanis, S. Papapoulos, J. Y. Reginster, R. Rizzoli, W. Dere, B. Mitlak, Y. Tsouderos, and S. Boonen, "Implications for fracture healing of current and new osteoporosis treatments: An ESCEO consensus paper," *Calcified Tissue International*, vol. 90, no. 5, pp. 343–353, 2012.
- [71] S. Toosi and J. Behravan, "Osteogenesis and bone remodeling: A focus on growth factors and bioactive peptides," *BioFactors*, vol. 46, pp. 326–340, may 2020.
- [72] J. C. Crockett, M. J. Rogers, F. P. Coxon, L. J. Hocking, and M. H. Helfrich, "Bone remodelling at a glance," *Journal of Cell Science*, vol. 124, pp. 991–998, apr 2011.
- [73] T. A. Einhorn and L. C. Gerstenfeld, "Fracture healing: mechanisms and interventions," *Nature Reviews Rheumatology*, vol. 11, pp. 45–54, jan 2015.
- [74] H. F. Pereira, I. F. Cengiz, F. S. Silva, R. L. Reis, and J. M. Oliveira, "Scaffolds and coatings for bone regeneration," *Journal of Materials Science: Materials in Medicine*, vol. 31, p. 27, mar 2020.
- [75] V. Wu, M. N. Helder, N. Bravenboer, C. M. ten Bruggenkate, J. Jin, J. Klein-Nulend, and E. A. J. M. Schulten, "Bone Tissue Regeneration in the Oral and Maxillofacial Region: A Review on the Application of Stem Cells and New Strategies to Improve Vascularization," *Stem Cells International*, vol. 2019, pp. 1–15, dec 2019.
- [76] H. C. Pape, A. Evans, and P. Kobbe, "Autologous Bone Graft : Properties and Techniques," vol. 24, no. 3, pp. 36–40, 2010.
- [77] L. Vidal, C. Kampleitner, M. Á. Brennan, A. Hoornaert, and P. Layrolle, "Reconstruction of Large Skeletal Defects: Current Clinical Therapeutic Strategies and Future Directions Using 3D Printing," *Frontiers in Bioengineering and Biotechnology*, vol. 8, feb 2020.
- [78] G. Fernandez de Grado, L. Keller, Y. Idoux-Gillet, Q. Wagner, A.-M. Musset, N. Benkirane-Jessel, F. Bornert, and D. Offner, "Bone substitutes: a review of their characteristics, clinical use, and perspectives for large bone defects management," *Journal of Tissue Engineering*, vol. 9, p. 204173141877681, jan 2018.
- [79] Ž. Perić Kačarević, P. Rider, S. Alkildani, S. Retnasingh, M. Pejakić, R. Schnettler, M. Gosau, R. Smeets, O. Jung, and M. Barbeck, "An introduction to bone tissue engineering," *The International Journal of Artificial Organs*, vol. 43, pp. 69–86, feb 2020.
- [80] A. Wubneh, E. K. Tsekoura, C. Ayrancı, and H. Uludag, "Acta Biomaterialia Current state of fabrication technologies and materials for bone tissue engineering," vol. 80, pp. 1–30, 2018.

- [81] J. R. Perez, D. Kouroupis, D. J. Li, T. M. Best, L. Kaplan, and D. Correa, "Tissue Engineering and Cell-Based Therapies for Fractures and Bone Defects," *Frontiers in Bioengineering and Biotechnology*, vol. 6, pp. 1–23, jul 2018.
- [82] H. Saijo, Y. Fujihara, Y. Kanno, K. Hoshi, and A. Hikita, "Clinical experience of full custom-made artificial bones for the maxillofacial region," *Regenerative Therapy*, vol. 5, pp. 72–78, 2016.
- [83] F. Luongo, F. G. Mangano, A. Macchi, G. Luongo, and C. Mangano, "Custom-Made Synthetic Scaffolds for Bone Reconstruction: A Retrospective, Multicenter Clinical Study on 15 Patients," *BioMed Research International*, vol. 2016, pp. 1–12, 2016.
- [84] C. K. Colton, "Implantable biohybrid artificial organs," *Cell Transplantation*, vol. 4, no. 4, pp. 415–436, 1995.
- [85] A. Moya, J. Paquet, M. Deschepper, N. Laroquette, K. Oudina, C. Denoeud, M. Bensidhoum, D. Logeart-Avramoglou, and H. Petite, "Human Mesenchymal Stem Cell Failure to Adapt to Glucose Shortage and Rapidly Use Intracellular Energy Reserves Through Glycolysis Explains Poor Cell Survival After Implantation," *STEM CELLS*, vol. 36, pp. 363–376, mar 2018.
- [86] C. Correia, W. L. Grayson, M. Park, D. Hutton, B. Zhou, X. E. Guo, L. Niklason, R. A. Sousa, R. L. Reis, and G. Vunjak-Novakovic, "In vitro model of vascularized bone: Synergizing vascular development and osteogenesis," *PLoS ONE*, vol. 6, no. 12, 2011.
- [87] A. J. Friedenstein, I. I. Piatetzky-Shapiro, and K. V. Petrakova, "Osteogenesis in transplants of bone marrow cells.," *Journal of embryology and experimental morphology*, vol. 16, pp. 381–90, dec 1966.
- [88] M. Dominici, K. L. Blanc, I. Mueller, F. C. Marini, D. S. Krause, R. J. Deans, A. Keating, D. J. Prockop, and E. M. Horwitz, "Minimal criteria for defining multipotent mesenchymal stromal cells . The International Society for Cellular Therapy position statement," vol. 8, no. 4, pp. 315–317, 2006.
- [89] K. W. Yong, J. R. Choi, J. Y. Choi, and A. C. Cowie, "Recent Advances in Mechanically Loaded Human Mesenchymal Stem Cells for Bone Tissue Engineering," *International Journal of Molecular Sciences*, vol. 21, p. 5816, aug 2020.
- [90] E. A. Jaffe, R. L. Nachman, C. G. Becker, and C. R. Minick, "Culture of Human Endothelial Cells Derived from Umbilical Veins. IDENTIFICATION BY MORPHOLOGIC AND IMMUNOLOGIC CRITERIA," *Journal of Clinical Investigation*, vol. 52, pp. 2745–2756, nov 1973.
- [91] I. Kocherova, A. Bryja, P. Mozdziak, A. Angelova Volponi, M. Dyszkiewicz-Konwińska, H. Piotrowska-Kempisty, P. Antosik, D. Bukowska, M. Bruska, D. Iżycki, M. Zabel, M. Nowicki, and B. Kempisty, "Human Umbilical Vein Endothelial Cells (HUVECs) Co-Culture with Osteogenic Cells: From Molecular Communication to Engineering Prevascularised Bone Grafts," *Journal of Clinical Medicine*, vol. 8, p. 1602, oct 2019.

[92] S. W. Sawyer, K. Zhang, J. A. Horton, and P. Soman, “Perfusion-based co-culture model system for bone tissue engineering,” *AIMS Bioengineering*, vol. 7, no. 2, pp. 91–105, 2020.

[93] J. Schindelin, I. Arganda-Carreras, E. Frise, V. Kaynig, M. Longair, T. Pietzsch, S. Preibisch, C. Rueden, S. Saalfeld, B. Schmid, J. Y. Tinevez, D. J. White, V. Hartenstein, K. Eliceiri, P. Tomancak, and A. Cardona, “Fiji: An open-source platform for biological-image analysis,” *Nature Methods*, vol. 9, no. 7, pp. 676–682, 2012.

[94] A. Nizet, E. Cavalier, P. Stenvinkel, M. Haarhaus, and P. Magnusson, “Bone alkaline phosphatase: An important biomarker in chronic kidney disease – mineral and bone disorder,” *Clinica Chimica Acta*, vol. 501, no. November 2019, pp. 198–206, 2020.

[95] F. Haasters, W. C. Prall, D. Anz, C. Bourquin, C. Pautke, S. Endres, W. Mutschler, D. Docheva, and M. Schieker, “Morphological and immunocytochemical characteristics indicate the yield of early progenitors and represent a quality control for human mesenchymal stem cell culturing,” *Journal of Anatomy*, vol. 214, no. 5, pp. 759–767, 2009.

[96] N. Herranz and J. Gil, “Mechanisms and functions of cellular senescence,” *Journal of Clinical Investigation*, vol. 128, no. 4, pp. 1238–1246, 2018.

[97] S. Sethe, A. Scutt, and A. Stolzing, “Aging of mesenchymal stem cells,” *Ageing Research Reviews*, vol. 5, no. 1, pp. 91–116, 2006.

[98] D. C. Colter, I. Sekiya, and D. J. Prockop, “Identification of a subpopulation of rapidly self-renewing and multipotential adult stem cells in colonies of human marrow stromal cells,” *Proceedings of the National Academy of Sciences*, vol. 98, pp. 7841–7845, jul 2001.

[99] D. Docheva, D. Padula, C. Popov, W. Mutschler, H. Clausen-Schaumann, and M. Schieker, “Researching into the cellular shape, volume and elasticity of mesenchymal stem cells, osteoblasts and osteosarcoma cells by atomic force microscopy: Stem Cells,” *Journal of Cellular and Molecular Medicine*, vol. 12, no. 2, pp. 537–552, 2008.

[100] J. Settleman, “Tension Precedes Commitment—Even for a Stem Cell,” *Molecular Cell*, vol. 14, pp. 148–150, apr 2004.

[101] C. Fehrer, R. Brunauer, G. Laschober, H. Unterluggauer, S. Reitinger, F. Kloss, C. Güly, R. Gaßner, and G. Lepperdinger, “Reduced oxygen tension attenuates differentiation capacity of human mesenchymal stem cells and prolongs their lifespan,” *Aging Cell*, vol. 6, pp. 745–757, aug 2007.

[102] W. L. Grayson, F. Zhao, B. Bunnell, and T. Ma, “Hypoxia enhances proliferation and tissue formation of human mesenchymal stem cells,” *Biochemical and Biophysical Research Communications*, vol. 358, no. 3, pp. 948–953, 2007.

[103] S. Y. Kwon, S. Y. Chun, Y. S. Ha, D. H. Kim, J. Kim, P. H. Song, H. T. Kim, E. S. Yoo, B. S. Kim, and T. G. Kwon, “Hypoxia Enhances Cell Properties of Human Mesenchymal Stem Cells,” *Tissue Engineering and Regenerative Medicine*, vol. 14, no. 5, pp. 595–604, 2017.

[104] M. A. Baxter, "Study of Telomere Length Reveals Rapid Aging of Human Marrow Stromal Cells following In Vitro Expansion," *Stem Cells*, vol. 22, pp. 675–682, sep 2004.

[105] N. Haque, M. T. Rahman, N. H. Abu Kasim, and A. M. Alabsi, "Hypoxic Culture Conditions as a Solution for Mesenchymal Stem Cell Based Regenerative Therapy," *The Scientific World Journal*, vol. 2013, pp. 1–12, 2013.

[106] M. Ejtehadifar, K. Shamsasenjan, A. Movassaghpoor, P. Akbarzadehlah, N. Dehdilani, P. Abbasi, Z. Molaeipour, and M. Saleh, "The effect of hypoxia on mesenchymal stem cell biology," *Advanced Pharmaceutical Bulletin*, vol. 5, no. 2, pp. 141–149, 2015.

[107] S. Bahsoun, K. Coopman, and E. C. Akam, "The impact of cryopreservation on bone marrow-derived mesenchymal stem cells: A systematic review," *Journal of Translational Medicine*, vol. 17, no. 1, 2019.

[108] T.-S. Li and E. Marbán, "Physiological Levels of Reactive Oxygen Species are Required to Maintain Genomic Stability in Stem Cells," *STEM CELLS*, vol. 23, pp. N/A–N/A, may 2010.

[109] J. C. Estrada, C. Albo, A. Benguría, A. Dopazo, P. López-Romero, L. Carrera-Quintanar, E. Roche, E. P. Clemente, J. A. Enríquez, A. Bernad, and E. Samper, "Culture of human mesenchymal stem cells at low oxygen tension improves growth and genetic stability by activating glycolysis," *Cell Death and Differentiation*, vol. 19, no. 5, pp. 743–755, 2012.

[110] A. T. Buizer, S. K. Bulstra, A. G. Veldhuizen, and R. Kuijer, "The balance between proliferation and transcription of angiogenic factors of mesenchymal stem cells in hypoxia," *Connective Tissue Research*, vol. 59, pp. 12–20, jan 2018.

[111] C. Holzwarth, M. Vaegler, F. Gieseke, S. M. Pfister, R. Handgretinger, G. Kerst, and I. Müller, "Low physiologic oxygen tensions reduce proliferation and differentiation of human multipotent mesenchymal stromal cells," *BMC Cell Biology*, vol. 11, no. 1, p. 11, 2010.

[112] J. Justesen, K. Stenderup, E. Eriksen, and M. Kassem, "Maintenance of Osteoblastic and Adipocytic Differentiation Potential with Age and Osteoporosis in Human Marrow Stromal Cell Cultures," *Calcified Tissue International*, vol. 71, pp. 36–44, jul 2002.

[113] A. Andrzejewska, R. Catar, J. Schoon, T. H. Qazi, F. A. Sass, D. Jacob, A. Blankenstein, S. Reinke, D. Krüger, M. Streitz, S. Schlick-eiser, S. Richter, N. Souidi, C. Beez, J. Kamhieh-Milz, U. Krüger, T. Zemojtel, K. Jürchott, D. Strunk, P. Reinke, G. Duda, G. Moll, and S. Geissler, "Multi-Parameter Analysis of Biobanked Human Bone Marrow Stromal Cells Shows Little Influence for Donor Age and Mild Comorbidities on Phenotypic and Functional Properties," *Frontiers in Immunology*, vol. 10, pp. 1–24, nov 2019.

[114] S. Zhou, J. S. Greenberger, M. W. Epperly, J. P. Goff, C. Adler, M. S. LeBoff, and J. Glowacki, "Age-related intrinsic changes in human bone-marrow-derived mesenchymal stem cells and their differentiation to osteoblasts," *Aging Cell*, vol. 7, pp. 335–343, jun 2008.

- [115] T. J. Block, M. Marinkovic, O. N. Tran, A. O. Gonzalez, A. Marshall, D. D. Dean, and X.-D. Chen, “Restoring the quantity and quality of elderly human mesenchymal stem cells for autologous cell-based therapies,” *Stem Cell Research & Therapy*, vol. 8, p. 239, dec 2017.
- [116] N. Xu, H. Liu, F. Qu, J. Fan, K. Mao, Y. Yin, J. Liu, Z. Geng, and Y. Wang, “Hypoxia inhibits the differentiation of mesenchymal stem cells into osteoblasts by activation of Notch signaling,” *Experimental and Molecular Pathology*, vol. 94, pp. 33–39, feb 2013.
- [117] R. Das, H. Jahr, G. J. van Osch, and E. Farrell, “The Role of Hypoxia in Bone Marrow–Derived Mesenchymal Stem Cells: Considerations for Regenerative Medicine Approaches,” *Tissue Engineering Part B: Reviews*, vol. 16, pp. 159–168, apr 2010.
- [118] E. Burian, F. Probst, B. Palla, C. Riedel, M. M. Saller, M. Cornelsen, F. König, M. Schieker, and S. Otto, “Effect of hypoxia on the proliferation of porcine bone marrow-derived mesenchymal stem cells and adipose-derived mesenchymal stem cells in 2- and 3-dimensional culture,” *Journal of Cranio-Maxillofacial Surgery*, vol. 45, no. 3, pp. 414–419, 2017.
- [119] F. Engin, Z. Yao, T. Yang, G. Zhou, T. Bertin, M. M. Jiang, Y. Chen, L. Wang, H. Zheng, R. E. Sutton, B. F. Boyce, and B. Lee, “Dimorphic effects of Notch signaling in bone homeostasis,” *Nature Medicine*, vol. 14, pp. 299–305, mar 2008.
- [120] D. C. Genetos, C. A. Toupadakis, L. F. Raheja, A. Wong, S. E. Panagiotakou, D. P. Fyhrie, G. G. Loots, and C. E. Yellowley, “Hypoxia decreases sclerostin expression and increases Wnt signaling in osteoblasts,” *Journal of Cellular Biochemistry*, vol. 23, no. 1, pp. n/a–n/a, 2010.
- [121] X. Yu, Q. Wan, X. Ye, Y. Cheng, J. L. Pathak, and Z. Li, “Cellular hypoxia promotes osteogenic differentiation of mesenchymal stem cells and bone defect healing via STAT3 signaling,” *Cellular & Molecular Biology Letters*, vol. 24, p. 64, dec 2019.
- [122] M. Zaim, S. Karaman, G. Cetin, and S. Isik, “Donor age and long-term culture affect differentiation and proliferation of human bone marrow mesenchymal stem cells.,” *Annals of hematology*, vol. 91, pp. 1175–86, aug 2012.
- [123] C. R. Ogando, G. A. Barabino, and Y. H. K. Yang, “Adipogenic and Osteogenic Differentiation of In Vitro Aged Human Mesenchymal Stem Cells,” *Methods in Molecular Biology*, vol. 2045, no. November 2018, pp. 107–117, 2019.
- [124] J. Bagge, L. C. Berg, J. Janes, and J. N. MacLeod, “Donor age effects on in vitro chondrogenic and osteogenic differentiation performance of equine bone marrow- and adipose tissue-derived mesenchymal stromal cells,” *BMC Veterinary Research*, vol. 18, no. 1, pp. 1–21, 2022.
- [125] W. C. Prall, M. M. Saller, A. Scheumaier, T. Tucholski, S. Taha, W. Böcker, and H. Polzer, “Proliferative and osteogenic differentiation capacity of mesenchymal stromal cells: Influence of harvesting site and donor age,” *Injury*, vol. 49, no. 8, pp. 1504–1512, 2018.

[126] G. Siegel, T. Kluba, U. Hermanutz-Klein, K. Bieback, H. Northoff, and R. Schäfer, “Phenotype, donor age and gender affect function of human bone marrow-derived mesenchymal stromal cells,” *BMC Medicine*, vol. 11, p. 146, dec 2013.

[127] P. Jia, H. Chen, H. Kang, J. Qi, P. Zhao, M. Jiang, L. Guo, Q. Zhou, N. D. Qian, H. B. Zhou, Y. J. Xu, Y. Fan, and L. F. Deng, “Deferoxamine released from poly(lactic-co-glycolic acid) promotes healing of osteoporotic bone defect via enhanced angiogenesis and osteogenesis,” *Journal of Biomedical Materials Research Part A*, vol. 104, pp. 2515–2527, oct 2016.

[128] W. C. Prall, F. Haasters, J. Heggebö, H. Polzer, C. Schwarz, C. Gassner, S. Grote, D. Anz, M. Jäger, W. Mutschler, and M. Schieker, “Mesenchymal stem cells from osteoporotic patients feature impaired signal transduction but sustained osteoinduction in response to BMP-2 stimulation,” *Biochemical and Biophysical Research Communications*, vol. 440, no. 4, pp. 617–622, 2013.

[129] T. Miyamoto, “Mechanism Underlying Post-menopausal Osteoporosis: HIF1 α is Required for Osteoclast Activation by Estrogen Deficiency,” *The Keio Journal of Medicine*, vol. 64, no. 3, pp. 44–47, 2015.

[130] Q. Zhao, X. Shen, W. Zhang, G. Zhu, J. Qi, and L. Deng, “Mice with increased angiogenesis and osteogenesis due to conditional activation of HIF pathway in osteoblasts are protected from ovariectomy induced bone loss,” *Bone*, vol. 50, pp. 763–770, mar 2012.

[131] P. Vrtačník, J. Zupan, V. Mlakar, T. Kranjc, J. Marc, B. Kern, and B. Ostanek, “Epigenetic enzymes influenced by oxidative stress and hypoxia mimetic in osteoblasts are differentially expressed in patients with osteoporosis and osteoarthritis,” *Scientific Reports*, vol. 8, p. 16215, dec 2018.

[132] J. Chen, L. Deng, C. Porter, G. Alexander, D. Patel, J. Vines, X. Zhang, D. Chasteen-Boyd, H.-J. Sung, Y.-P. Li, A. Javed, S. Gilbert, K. Cheon, and H.-W. Jun, “Angiogenic and Osteogenic Synergy of Human Mesenchymal Stem Cells and Human Umbilical Vein Endothelial Cells Cocultured on a Nanomatrix,” *Scientific Reports*, vol. 8, p. 15749, dec 2018.

[133] Y. Xue, Z. Xing, S. Helle, K. Arvidson, and K. Mustafa, “Endothelial cells influence the osteogenic potential of bone marrow stromal cells,” *BioMedical Engineering OnLine*, vol. 8, no. 1, p. 34, 2009.

[134] C. Boulard, P. Philippart, D. Dequanter, F. Corrillon, I. Loeb, D. Bron, L. Lagneaux, and N. Meuleman, “Cross-Talk Between Mesenchymal Stromal Cells (MSCs) and Endothelial Progenitor Cells (EPCs) in Bone Regeneration,” *Frontiers in Cell and Developmental Biology*, vol. 9, no. May, pp. 1–17, 2021.

[135] M. Grellier, L. Bordenave, and J. Amédée, “Cell-to-cell communication between osteogenic and endothelial lineages: implications for tissue engineering,” *Trends in Biotechnology*, vol. 27, pp. 562–571, oct 2009.

[136] F. Villars, L. Bordenave, R. Bareille, and A. J., “Effect of human endothelial cells on Human Bone Marrow Stromal Cell phenotype: Role of VEGF?,” *Journal of Cellular Biochemistry*, vol. 79, pp. 672–685, dec 2000.

- [137] J. Ma, J. J. van den Beucken, F. Yang, S. K. Both, F.-Z. Cui, J. Pan, and J. A. Jansen, “Coculture of Osteoblasts and Endothelial Cells: Optimization of Culture Medium and Cell Ratio,” *Tissue Engineering Part C: Methods*, vol. 17, pp. 349–357, mar 2011.
- [138] X. Liu, W. Chen, C. Zhang, W. Thein-Han, K. Hu, M. A. Reynolds, C. Bao, P. Wang, L. Zhao, and H. H. Xu, “Co-Seeding Human Endothelial Cells with Human-Induced Pluripotent Stem Cell-Derived Mesenchymal Stem Cells on Calcium Phosphate Scaffold Enhances Osteogenesis and Vascularization in Rats,” *Tissue Engineering Part A*, vol. 23, pp. 546–555, jun 2017.
- [139] Y. Yan, H. Chen, H. Zhang, C. Guo, K. Yang, K. Chen, R. Cheng, N. Qian, N. Sandler, Y. S. Zhang, H. Shen, J. Qi, W. Cui, and L. Deng, “Vascularized 3D printed scaffolds for promoting bone regeneration,” *Biomaterials*, vol. 190-191, pp. 97–110, jan 2019.
- [140] S. Zhang, M. Zhou, Z. Ye, Y. Zhou, and W.-S. Tan, “Fabrication of viable and functional pre-vascularized modular bone tissues by coculturing MSCs and HUVECs on microcarriers in spinner flasks,” *Biotechnology Journal*, vol. 12, p. 1700008, aug 2017.
- [141] Y. Zhang, W. Yang, A. Devit, and J. J. van den Beucken, “Efficiency of coculture with angiogenic cells or physiological BMP-2 administration on improving osteogenic differentiation and bone formation of MSCs,” *Journal of Biomedical Materials Research Part A*, vol. 107, pp. 643–653, mar 2019.
- [142] S. Fuchs, A. Hofmann, and C. J. Kirkpatrick, “Microvessel-Like Structures from Outgrowth Endothelial Cells from Human Peripheral Blood in 2-Dimensional and 3-Dimensional Co-Cultures with Osteoblastic Lineage Cells,” *Tissue Engineering*, vol. 13, pp. 2577–2588, oct 2007.
- [143] K. Wang, R.-Z. Lin, and J. M. Melero-Martin, “Bioengineering human vascular networks: trends and directions in endothelial and perivascular cell sources.,” *Cellular and molecular life sciences : CMLS*, vol. 76, pp. 421–439, feb 2019.
- [144] B. Zhang, S. Yang, Y. Zhang, Z. Sun, W. Xu, and S. Ye, “Co-culture of mesenchymal stem cells with umbilical vein endothelial cells under hypoxic condition,” *Journal of Huazhong University of Science and Technology [Medical Sciences]*, vol. 32, pp. 173–180, apr 2012.
- [145] N. Koike, D. Fukumura, O. Gralla, P. Au, J. S. Schechner, and R. K. Jain, “Creation of long-lasting blood vessels,” *Nature*, vol. 428, pp. 138–139, mar 2004.
- [146] F. Xing, Z. Xiang, P. M. Rommens, and U. Ritz, “3D Bioprinting for Vascularized Tissue-Engineered Bone Fabrication,” *Materials*, vol. 13, p. 2278, may 2020.
- [147] F. Xing, Z. Xiang, P. M. Rommens, and U. Ritz, “3D Bioprinting for Vascularized Tissue-Engineered Bone Fabrication,” *Materials*, vol. 13, p. 2278, may 2020.

7 Supplementary data

7.1 A. Influence of the donor age on proliferation, colony forming unit capacity and osteogenic differentiation capacity

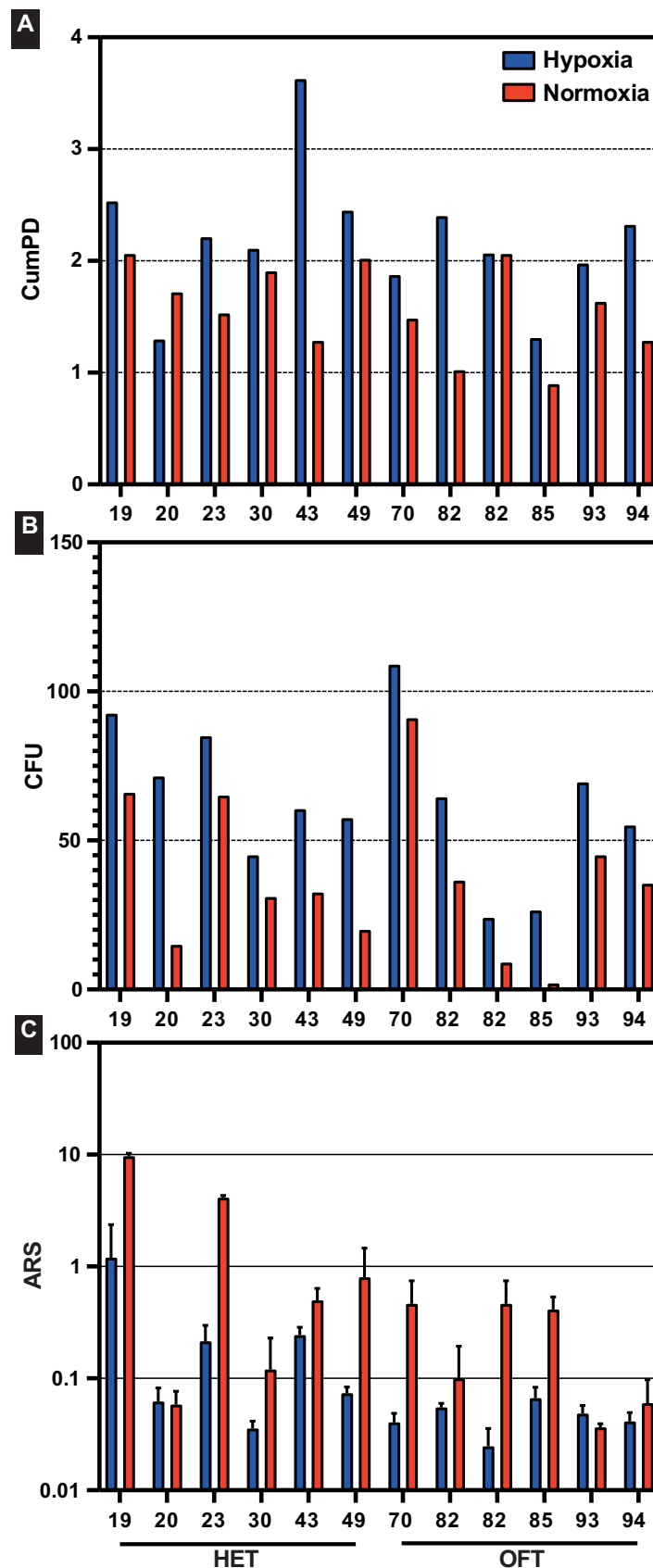


Figure 15: A: Cum PD in hypoxia and normoxia in relation to donor age. B: CFU in hypoxia and normoxia in relation to donor age. C: ARS in hypoxia and normoxia in relation to donor age.

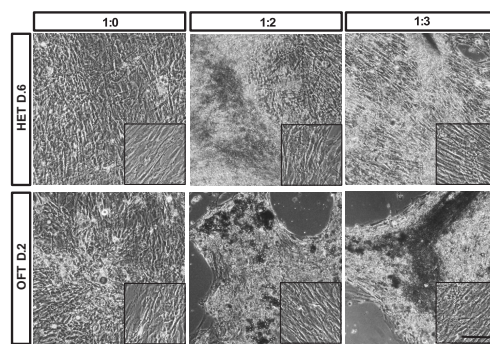


Figure 16: HET hMSCs (HET D.6) and OFT group (OFT D.2) in co-cultures (hSMS: hU-VEC) during osteogenic differentiation with control group in the lower right corner. The osteogenic differentiated co-cultures show small holes, not filled with cells. These holes are not shown in the control groups. Bar equals 100 μ m

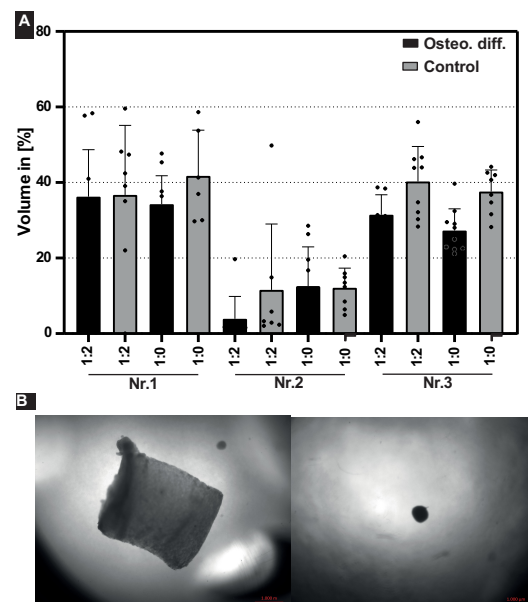


Figure 17: A: Scaffold size of the different donors after osteogenic differentiation and control. B: Seeded scaffold of hMSCs of donor 2 ratio 1:2 undergoing osteogenic differentiation on the first day (left image) and after 14 days of seeding (right image). Scaffold size changed tremendously over time. Bar equals 1000 μ m

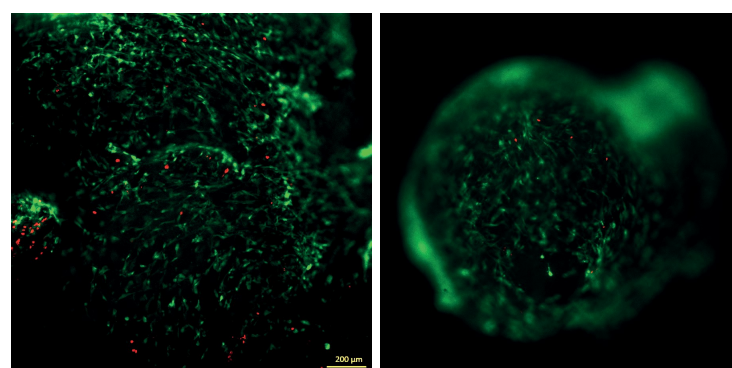


Figure 18: Scaffold seeded with a ratio of 1:2 with hMSCs of donor 10 after 7 days, before initiating the osteogenic differentiation. Living cells are stained by fluorescent metabolite fluorescein (green) and dead cells stained by propidium iodide (red). Many cells were still vital after 7 days of cell culture. Bar equals 1000 μ m

8 Appendix

Medium	Firm
ALP	Alkaline phosphatase
ARS	Alizarin Red staining
AUC	Area under the curve
BMD	Bone mineral density
BMP-2	Bone morphogenetic protein 2
BMP-4	Bone morphogenetic protein 4
BTE	Bone tissue engineering
CFU	Colony forming units
CSF-1	Colony-stimulating factor 1
Cum PD	Cumulative population doubling
DXA	Dual x-ray absorptiometry
EC	endothelial cells
ECM	Extracellular matrix
ET1	endothelin-1
FBS	Fetal bovin serum
FGF	Fibroblast growth factor
FRAZ	Fracture Risk Assessment Tool
GF	Gas foaming
HET	high-energy trauma
HIF	Hypoxia-inducible factor
hMSC	Human mesenchymal stem cells
HRE	Hypoxia-response element
IGF-1	Insulin-like-growth-factor 1
IL-1	Interleukin-1
IL-6	Interleukin-6
MSC	Mesenchymal stem cells
MT1-MMP	Membrane type-1 matrixmetalloproteinase
OD	Osteogenic differentiation
OFT	osteoporotic-fracture trauma
OPG	osteoprotegerin
QCT	Quantitative computed tomography
QUIS	Quantitative ultrasound
RANKL	Receptor activator of NF- κ B ligand
RUNx2	Runt-related transcription factor 2
SD	Standard deviation
SERM	Selective estrogen-receptor modulator
TNF-upalpha	Tumor necrosis factor-upalpha
UVEC	Umbilical vein endothelial cells
VEGF	Vascular endothelial growth factor

Table 4: Cell culture medium

8.1 List of materials and chemicals

Medium	Firm
Dulbecco´s modified eagle´s medium DMEM	Gibco, Thermo Fischer, USA
Endothelial cell growth medium ECGM I	Promocell, Germany
Endothelial cell growth medium ECGM II	Promocell, Germany
Minimum essential medium upalpha-MEM	Gibco, Thermo Fischer, USA
Supplement mix I C-39215	Promocell, Germany
Supplement mix II C-39216	Promocell, Germany

Table 5: Cell culture medium

Laboratory equipment	Firm
Cell culture flask T25,T75,T150	Nunc, Thermo Fisher, USA
Centrifuge Universal 16R	Hettich Zentrifugen, Germany
ELISA reader	Multiskan FC, Thermo Fisher, USA
Incubator (Hypoxic 5% O_2)	MCO-5M, Sanyo, Germany
Incubator (Normoxic 21% O_2)	Memmert electronic, Germany
Microscope Axio Observer Z1	Zeiss, Germany
Microscope Axiovert 40 CFL	Zeiss, Germany
Microscope Leica M165 FC	Leica, Germany
pH indicator bar	Merck, Germany
Thermomixer compact	Eppendorf, Germany

Table 6: Laboratory equipment

Software	Firm
Adobe Illustrator CS6	Version 16.0.0 x64, Adobe System Inc., USA
Adobe Photoshop CS6	Version 13.0 x64, Adobe System Inc., USA
Graphpad Prism 5	Version 5.02, Graphpad Software Inc., USA
ImageJ	Version 1.51n (Java 1.8.0_66 // 64-bit)
ZEN lite 2012	Version 1.1.2.0, Zeiss, Germany

Table 7: Software

Chemicals	Firm
1 % Penicillin/Streptomycin P/S	Biochrom GmbH, Germany
1% fungicide	Patricin, Biochrom GmbH,Germany
10% Fetal bovin serum	, Sigma-Aldrich, USA
Acetic acid	Sigma-Aldrich,USA
Alizarin Red S	Sigma-Aldrich, USA
Ammonium acetate	Sigma-Aldrich, St.Louis, Missouri,USA
Ammonium hydroxide solution	Sigma-Aldrich, USA
Aqua dest.	Gibco, Thermo Fisher, USA
BMP-2	MACS Miltenyi Biotec, Bergisch Gladbach, Germany
Collagenese II 260 U/mg	Worthington Biocemial Corporation, Lakewood, USA
Dexamethasone	Sigma-Aldrich, USA
Dimethylsulfoxid	Carl Roth GmbH, Germany
Eosin	Sigma-Aldrich, USA
Hydrochloric acid	Merck, Darmstadt, Germany
L-ascorbic acid	Sigma-Aldrich, USA
Magnesium chloride	Carl Roth, Karlsruhe Germany
NTB/BCIP	Sigma-Aldrich, USA
Paraformaldehyd	Merck, Darmstadt, Germany
Phosphate-buffered saline	Thermo Fisher, USA
Polyvenyl alcohol	Sigma-Aldrich, USA
Sodium chloride	Carl Roth, Karlsruhe Germany
β-glycerolphosphate	Sigma-Aldrich, USA
Trishydroxymethylaminomethan	Sigma-Aldrich, USA
Trypan blue Stain 0,4%	Invitrogen, Thermo Fischer, USA
Trypsin/EDTA Solution 10x	Biochrom GmbH, Germany
Tween-20	Sigma-Aldrich, USA

Table 8: Chemicals

List of Figures

1	Schematic overview of the development of the bone and vascular system. A. Progenitor cells differentiate into chondrocytes and form a cartilage model with the shape of the future bone. B. Chondrocytes in the center become hypertrophic and mesenchymal stem cells in the perichondrium differentiate into osteoprogenitor cells, forming the primary ossification center (POC). Osteoprogenitor cells and chondrocytes increase VEGF expression through transcription factors (Runx2 and Osterix). VEGF stimulates the neovascularization of the cartilage model. The invasion of new blood vessels increases the supply of oxygen, nutrients and growth factor, thereby promoting mineralization. C. With the invasion of the blood vessels, osteoprogenitors move along to the changing site. Cartilage is resorbed by osteoclasts and new bone is formed by osteoblasts. With the ongoing process, a bone marrow cavity is produced. Concurrently, the epiphyseal growth plates, which are responsible for longitudinal growth, are formed. Perichondrium is transformed into periosteum. D. Due to the longitudinal growth and the avascularity of the growth plate, cells encounter a hypoxic state. The latter causes the stabilization of HIF and increases the expression of VEGF by chondrocytes. The invasion of vessels, which contribute to the formation of a secondary ossification center (SOC), is facilitated.	4
2	Exemplary microscopy of the morphological changes in hMSCs from the HET (A) and OFT (B) group in normoxia and hypoxia after 10 and 20 days. Macroscopically, there were no significant differences in cell morphology, neither comparing normoxia to hypoxia, nor when comparing the HET group to the OFT group. A. HET donor 5 B. OFT donor 4, Bar equals 20 μ m	17

3 A and C: Quantification of cell area in normoxia and hypoxia for all HET and OFT groups. Day 10 (A): Comparing hypoxic to normoxic cell culture conditions, a significant change in area was observed for the HET group ($p<0.0001$) and a non-significant change for the OFT group ($p>0.999$). Comparing the HET to the OFT group in normoxia, a significant change was observed, but a non-significant difference was observed in hypoxia (normoxia $p<0.0001$, hypoxia $p>0.999$). Day 20 (B): Comparing hypoxia to normoxia for the HET group, the change was significant (HET $p=0.0002$). For the OFT group, the change was not significant ($p=0.0762$). Comparing HET to the OFT group, a significant change was not seen in either normoxia or hypoxia (normoxia $p>0.999$, hypoxia $p>0.999$). Comparison of the area measurements on day 10 and day 20 for the HET group cultured in normoxia, showed a significant change ($p=0.0012$). In hypoxia, no significant change was seen ($p>0.999$). Comparing the area measurements on day 10 to day 20, no significant change was seen for the OFT group (normoxia $p>0.999$, hypoxia $p>0.999$) B and D: Quantification of the aspect ratio in normoxia and hypoxia on day 10 and day 20, for both the HET and OFT groups. Comparing hypoxia to normoxia, no significant change was calculated for the HET or OFT groups. Only comparison of day 10 to day 20 for the OFT group in normoxia showed a significant change ($p=0.0092$). Box and whisker plot (min and max point), with median (line) and mean (+). Only significant changes are represented graphically.....19

4 CumPD of all donors in the HET group (A) and OFT group (B) in normoxic and hypoxic cell culture conditions. For almost all donors (except HET D.6 and OFT D.4) proliferation was higher in hypoxic cell culture conditions. For most donors in the HET and the OFT groups, proliferation was similar until day 5. After 5 days, proliferation in hypoxic cell culture conditions continued, whereas proliferation reduced in normoxic culture conditions. This effect was noted especially for donor D.1 in the HET group, where proliferation almost doubled in hypoxic cell culture conditions. For all the other donors in the HET group, except D.6, proliferation was improved in hypoxic cell culture conditions. A similar effect was seen for the OFT group. For several donor samples (D.2 and D.5) in the OFT group, cells ceased growth in normoxic conditions, whereas they kept growing in hypoxic conditions. Comparing the proliferation capacity of the HET to the OFT group, a slightly higher proliferation capacity was observed for the HET group.....20

5 A: CumPD comparison between the HET group and the OFT group in normoxic and hypoxic cell culture conditions over a period of 20 days. HET donor samples reached a mean cumPD of 1.75 ± 0.30 in normoxia and a mean cumPD of 2.37 ± 0.75 in hypoxia. (p=0.174). For the OFT group, there was a mean cumPD of 1.39 ± 0.42 in normoxic conditions and a mean cumPD of 1.99 ± 0.39 in hypoxic conditions (p=0.199). B: CumPD pooled in the HET and OFT groups and comparison of normoxia to hypoxia. Under both conditions, although HET donor samples performed better than OFT donor samples, the results were non-significant (normoxia: p=0.612, hypoxia p=0.565). The only significant change was seen when comparing the HET group in hypoxia to the OFT group in normoxia (p=0.014). Graph: Box and whisker plot (min and max point) with median (line) and mean (+). Only significant changes are represented graphically. 21

6 A: Each donor sample in the HET and OFT groups is presented individually. The AUC is shown for both culture conditions (normoxia and hypoxia). In particular, donor 1 in the HET group displayed a considerable difference between normoxia and hypoxia, showing a higher AUC in hypoxia. On the other hand, donor 6 in the HET group showed a slight decrease in hypoxia. For the OFT group, with the exception of donor 4, all donors showed a better growth potential in hypoxic cell culture conditions. B: AUC comparing HET and OFT groups in normoxic and hypoxic cell culture conditions after 20 days of cell culture. Significant changes were not found in the HET or in the OFT group, when comparing the AUC in hypoxic to normoxic cell culture conditions (HET p=0.135, OFT p=0.0681). However there was a tendency towards higher proliferation capacity in hypoxia. When comparing the groups (HET to OFT), no significant changes were observed (normoxia: p=0.2876, hypoxia: p=0.3478). Graph: Box and whisker plot (min and max point) with median (line) and mean (+). Only significant changes are represented graphically..... 22

7 CFU (A) and efficiency (B) of the HET and OFT groups in hypoxia and normoxia. A: The HET and the OFT group show a higher number of colonies in hypoxic cell culture conditions. B: As for the efficiency, the HET group revealed a non-significant change when comparing the two culture conditions (normoxia/hypoxia) (p=0.221), as did the OFT group (p=0.502). Comparing the HET to the OFT group, a non-significant change was observed (normoxia: p=0.999, hypoxia: p=0.900). Graph: Box and whisker plot (min and max point) with median (line) and mean (+). Only significant changes are represented graphically. 23

8 Exemplary microscopy images of osteogenic differentiation and ARS in the HET group and OFT group. The images in the right corners represent the corresponding controls (not induced to osteogenic differentiation). All hMSCs were cultured in normoxia and hypoxia. Microscopically almost all donors in the HET group show a homogeneous matrix and staining in normoxia. Only D.3 showed a weaker staining signal. In hypoxia, they showed less mineralization. Macroscopically the OFT group showed less mineralization in hypoxic conditions than in normoxic cell culture conditions. Comparing the HET group to the OFT group, especially in normoxia, the staining signal seemed stronger for the HET group. Only a slight difference (HET/OFT) was noticeable in hypoxia. Bar equals 20 μ m.....24

9 A: Alizarin Red quantification of all hMSCs donors in normoxic and hypoxic cell cultures. Except for HET D.6 and OFT D.6 which showed a decrease of the ARS concentration, all donors displayed a tendency towards a better osteogenic differentiation in normoxic cell culture conditions. B: Alizarin Red staining quantification of the HET and OFT groups in normoxic and hypoxic cell culture conditions and in the associated control group. The HET group showed a mean ARS concentration of 2.544 ± 3.808 mM in normoxia and 0.305 ± 0.448 mM in hypoxia. The OFT group presented a mean ARS concentration of 0.189 ± 0.194 mM in normoxia and an average ARS concentration of 0.046 ± 0.014 mM in hypoxia. In both conditions, control groups produced ARS concentration close to zero (normoxia: 0.0031 ± 0.017 mM, hypoxia: 0.041 ± 0.016 mM). Comparing the osteogenic differentiated group to the control group, a significant change was observed in normoxia for the HET group ($p=0.005$). For the OFT group, the change was not significant ($p=0.999$). A non-significant ARS concentration was calculated when comparing the osteogenic differentiation group to the control group in hypoxia (HET: $p=0.998$; OFT $p=0.990$). Comparing HET to the OFT group in normoxia there was a significant difference ($p=0.039$), but the difference was not significant in hypoxia ($p=0.999$). Graph: A: Individual values paired in normoxia and hypoxia. B: Box and whisker plot (min and max point) with median (line) and mean (+). Only significant changes are represented graphically. 26

10 Increase or decrease of the different donor samples in normoxic compared to hypoxic cell cultures. A. All donors, except HET D.6 and OFT D.6, showed an increased mineralization in normoxic cell culture conditions. B. Comparison the two major groups HET and OFT ($p=0.334$). Graph: Bar plot (A) and box plot (B) with min. and max. point, median (line) and mean (+). Only significant changes are represented graphically. 27

11 Exemplary microscopy images of ARS of HET donor samples (A) and OFT donor samples (B) at different ratios with hUVECs during osteogenic differentiation. Macroscopically, mineralization was produced in all three ratios (hMSCs:hUVECs). Increased mineralization was observed for co-cultures (hMSCs:hUVECs) in ratios of 1:2 and 1:3. Bar equals 1000 μ m 28

12 A: ARS quantification of all donor samples in monocultures and co-culture with hUVECs in different ratios undergoing osteogenic differentiation. For most donor samples, in both the HET and the OFT group, co-cultures enhanced the mineralization process. For several donors this enhancement was especially notable in the 1:2 ratio, (e.g. HET D.1, HET D.6 and OFT D.1, OFT D.2, OFT D.3). However, HET D.4 showed decreased mineralization in both ratios. B: HET donor monocultures a mean ARS concentration of 0.230 ± 0.130 mM was calculated. HET donor co-cultures a mean ARS concentration of 0.300 ± 0.232 mM at a ratio of 1:2 and a mean ARS concentration of 0.256 ± 0.144 mM at a ratio of 1:3 was calculated. At all three ratios, ARS concentration calculated for the control groups were close to zero (1:0: 0.016 ± 0.024 mM, 1:2: 0.011 ± 0.011 mM, 1:3: 0.007 ± 0.003 mM). Comparison of the HET osteogenic differentiated group to the HET control group showed a significant difference for all three ratios (1:0: $p=0.0094$, 1:2: $p=0.0152$ 1:3: $p=0.0022$). Comparison of the osteogenetic differentiation ARS concentrations showed no significant difference in neither the HET 1:0 to the 1:2 ($p=0.985$), the HET 1:0 to 1:3 ($p>0.999$), nor the HET 1:2 to the 1:3 group ($p=0.999$). OFT group monocultures a mean ARS concentration of 0.146 ± 0.138 mM was calculated. OFT group co-cultures a mean AR of 0.256 ± 0.216 mM at a ratio of 1:2 and a mean AR of 0.255 ± 0.178 mM at a ratio of 1:3 was calculated. Comparison of the ARS concentration of the osteogenic differentiated OFT group to the control group a difference was shown (1:0: $p=0.420$, 1:2: $p=0.0051$, 1:3: $p=0.0048$). ARS concentration was not significantly different when comparing the OFT 1:0 to the 1:2 ($p=0.829$), the 1:0 to 1:3 ($p=0.832$), or the 1:2 to 1:3 group ($p>0.999$). When comparing the HET to the OFT group, there was no significant difference ($p=0.393$) in osteogenic differentiation potential at the ratio of 1:0, the ratio of 1:2 ($p=0.7399$) or at the ratio of 1:3 ($p=0.9969$). A wide scattering of the different ARS concentrations of the donors is observed. Graph A: Individual values connected by line at different ratios B: Box and whisker plot (min and max point) with median (line) and mean (+). Only significant changes are represented graphically..... 30

13 A: Measurement of increase or decrease in osteogenic differentiation potential, comparing monocultures at a ratio of 1:0 to co-cultures at ratios of 1:2 and 1:3. The HET group (A) showed a positive influence of osteogenic differentiation in the co-cultures for several donor samples (e.g: HET D.3 and D.6). However, some donor samples (e.g: HET D.4 and D.5) showed a lowered or unaltered potential. The OFT group was positively influenced in co-cultures for all donor samples, except one (OFT D.5 at ratio 1:3) B: When HET and OFT donors were paired into groups, a non-significant change was seen for the HET group ($p=0.904$) when comparing osteogenic differentiation potential in co-cultures at 1:2 and 1:3 ratio. The same result was seen for the OFT group ($p=0.993$), whereby there was a non-significant difference when comparing 1:2 and 1:3 ratio. Comparing the HET group to the OFT group a significant change was not observed in either 1:2 or the 1:3 groups ($p=0.362$ at ratio 1:2, $p=0.254$ at ratio 1:3). Graph: Box and whisker plot (min and max point) with median (line) and mean (+). Only significant changes are represented graphically 31

14 Exemplary microscopy images on day 14 of osteogenic differentiation, presenting hUVECs morphology in co-culture (1:2, 1:3) A. HET D.4 B. OFT D.2. During osteogenic differentiation cell formation (A and B) showed an increased accumulation and the cell structure seemed rounder, whereas hUVECs in the control group expanded more and the cell structure appeared more flattened. Bar equals 100 μ m 32

15 A: Cum PD in hypoxia and normoxia in relation to donor age. B: CFU in hypoxia and normoxia in relation to donor age. C: ARS in hypoxia and normoxia in relation to donor age 52

16 HET hMSCs (HET D.6) and OFT group (OFT D.2) in co-cultures (hSMS: hUVEC) during osteogenic differentiation with control group in the lower right corner. The osteogenic differentiated co-cultures show small holes, not filled with cells. This holes are not shown in the control groups. Bar equals 100 μ m 53

17 A: Scaffold size of the different donors after osteogenic differentiation and control. B: Seeded scaffold of hMSCs of donor 2 ratio 1:2 undergoing osteogenic differentiation on the first day (left image) and after 14 days of seeding (right image). Scaffold size changed tremendously over time. Bar equals 1000 μ m 53

18 Scaffold seeded with a ratio of 1:2 with hMSCs of donor 10 after 7 days, before initiating the osteogenic differentiation. Living cells are stained by fluorescent metabolite fluorescein (green) and death cells stained by propidium iodides (red). Many cells were still vital after 7 days of cell culture. Bar equals 1000 μ m 53

List of Tables

1	Cell material used in the experiment setup	10
2	Experiment 1 set up	15
3	Experiment 2 Set up.....	15
4	Cell culture medium	54
5	Cell culture medium	55
6	Laboratory equipment.....	55
7	Software.....	55
8	Chemicals	56

9 Acknowledgments

I would like to extend my sincere thanks to Prof. Böcker for providing me with the topic.

Words cannot express my gratitude to Dr.rer.nat Maximillian Saller and Dr. rer.nat Veronika Schönitzer for their invaluable patience, feedback and immense insight into fundamental research.

I also could not have undertaken this journey without the whole Experimed team, especially to PD Dr. Aszódi for providing the access to his lab and to Sebastian Reiprich, who generously provided knowledge and expertise.

I am also grateful to my boyfriend for his editing help, late-night feedback sessions, and moral support.

Lastly, I would be remiss in not mentioning my family, especially my parents. Their belief in me has kept my spirits and motivation high during this process.

**Eidesstattliche Versicherung**

Kohll, Céline

Name, Vorname

Ich erkläre hiermit an Eides statt, dass ich die vorliegende Dissertation mit dem Titel

**Influence of hypoxia and vascularization on the osteogenic differentiation and
mineralization capacity of primary osteoporotic human mesenchymal stem cells**

selbstständig verfasst, mich außer der angegebenen keiner weiteren Hilfsmittel bedient und alle Erkenntnisse, die aus dem Schrifttum ganz oder annähernd übernommen sind, als solche kenntlich gemacht und nach ihrer Herkunft unter Bezeichnung der Fundstelle einzeln nachgewiesen habe.

Ich erkläre des Weiteren, dass die hier vorgelegte Dissertation nicht in gleicher oder in ähnlicher Form bei einer anderen Stelle zur Erlangung eines akademischen Grades eingereicht wurde.

München, 26.07.2025

Ort, Datum

Céline Kohll

Unterschrift Céline Kohll

**Erklärung zur Übereinstimmung der gebundenen Ausgabe der Dissertation
mit der elektronischen Fassung**

Kohll, Céline

Name, Vorname

Hiermit erkläre ich, dass die elektronische Version der eingereichten Dissertation mit dem Titel:

Influence of hypoxia and vascularization on the osteogenic differentiation and mineralization capacity of primary osteoporotic human mesenchymal stem cells

in Inhalt und Formatierung mit den gedruckten und gebundenen Exemplaren übereinstimmt.

München, 26.07.2025

Ort, Datum

Céline Kohll

Unterschrift Céline Kohll